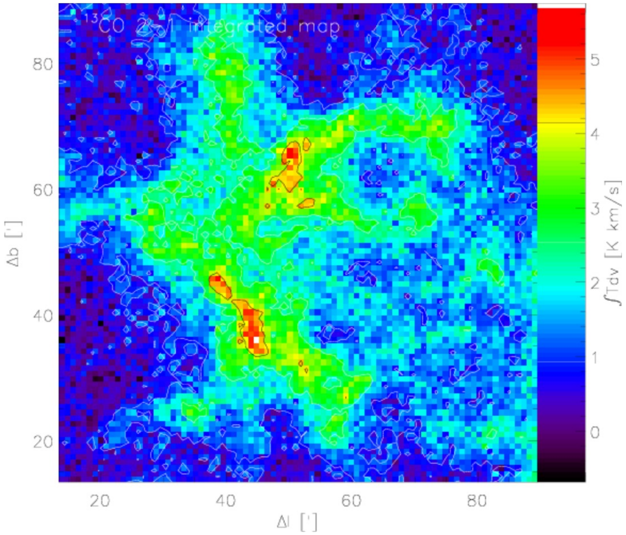

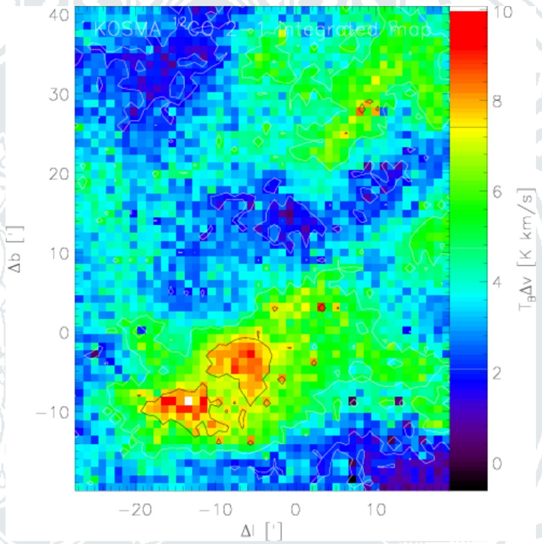

Characterizing interstellar cloud turbulence

Volker Ossenkopf-Okada

KOSMA
(Kölner Observatorium für SubMm Astronomie),
I. Physikalisches Institut, Universität zu Köln

ph1 Universität zu Köln

Overview

- Motivation
- What is turbulence?
  - Reynolds numbers
  - The turbulent energy cascade
  - Kolmogorov vs. Burgers'
- Comparing turbulence in observations and simulations
  - Velocity scaling
  - Column-density probability distribution functions (PDFs)
  - Spatial scaling: Δ-variance
  - Filaments
- Conclusions

The problem

Structure formation in the ISM:

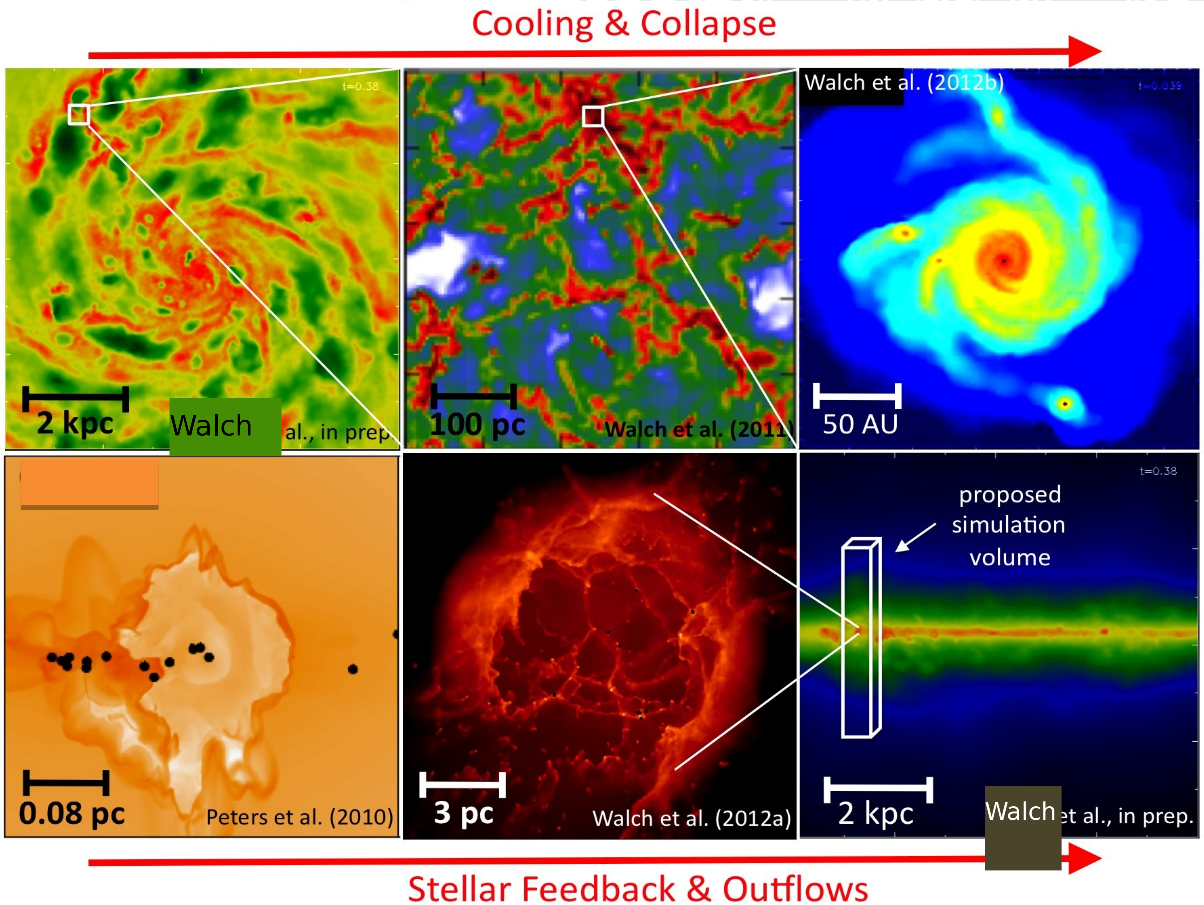

SILCC (Walch et al. 2016)

- How does the ISM structure control star-formation?
- How do young stars structure their environment?

→ What is systematics? What is the role of turbulence?

Understand the nature of structure formation

Systematic

- spiral arms
- shells
- outflows
- disks

Turbulent

- filaments
- shock networks
- clump hierarchies

How to distinguish?

Systematic:

- anisotropy
- pronounced size scales
- structured line profiles

Turbulent:

- isotropy
- fractal (multifractal) laws
- smooth line profiles

Quantify transition

→ Learn about scales and processes

Systematic:

- instabilities
- ordered gravitational collapse
- magnetic fields
- equation of state
- viscosity

Turbulent:

- energy cascade
- turbulent gravitational collapse
- (M)HD waves
- structure formation

Criterion for turbulence

- **Reynolds number**

$$\mathrm{Re} = \frac{LV}{\nu} \gg 1$$

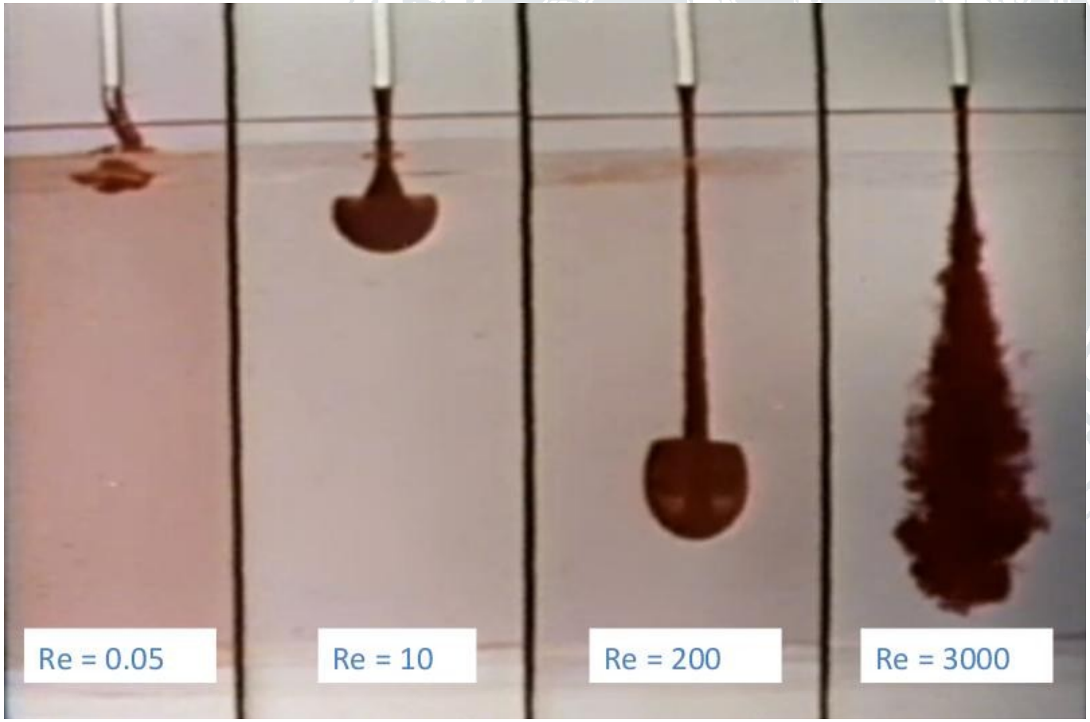

Taylor (1964)

- Geometric description of turbulent structure impossible
  → **Statistical description**

- **Interstellar medium:**
  - Diffuse interstellar clouds: $\mathrm{Re} \approx 10^5$
  - Molecular clouds: $\mathrm{Re} \approx 10^7$
  - **Every motion leads to turbulence**
  - **Every instability induces turbulence**

→ **The ISM is always turbulent!**

a) Kolmogorov turbulence (eddy theory):

- **Eddies form energy cascade of motions with different size:**

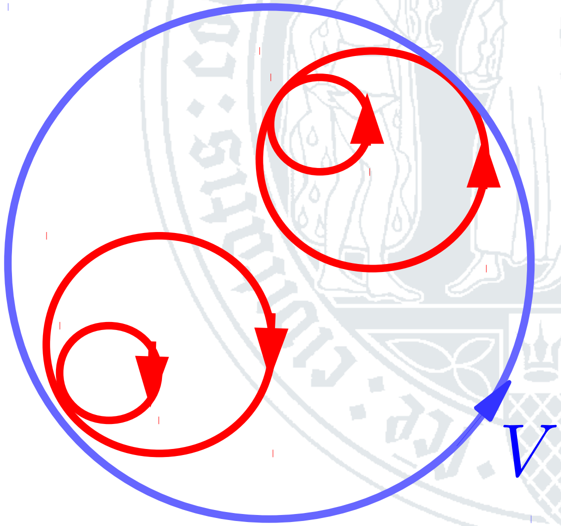

- Eddy with size l and velocity v :
  - Kinetic energy density: $e(l) = \frac{1}{2}\rho v^2$
- Energy cascade
  - Injection of motions on largest scale L (velocity V)
  - Dissipation of velocities at small scales by kinematic viscosity ν
  - Transfer of energy from large eddies to smaller eddies

Energy cascade

- **Energy transfer to smaller eddies**
  - At eddy time scale: $\tau_l = l/v$
  - Gives energy transfer rate: $\dot{e} = \frac{\rho}{2} v^2 \times \frac{\rho}{\tau_l} = \frac{1}{2} v^2 \times \frac{v}{l} = \rho \frac{v^3}{2l}$
- **But:** Energy is not injected/removed at scale l within the cascade, but only injected at scale L and removed at dissipation scale l_s

  → **Transfer rate $\dot{e}$ must not depend on l :** $\dot{e} = \mathrm{const.}$

  → $v(l) \propto l^{1/3}$

  Kolmogorov scaling law

- **Termination of cascade by viscosity at scale:** $l_s = \frac{L}{(\mathcal{R}e/2)^{3/4}}$
  - $\mathcal{R}e$ measures the difference in eddy size between injection and dissipation scale

In Fourier space

- **Description of eddies by wave numbers** $\vec{k} = \frac{2\pi}{|l^2|}\vec{l}$
  - Kolmogorov turbulence $v \propto l^{1/3} \longrightarrow v(|\vec{k}|) = v(k) \propto k^{-1/3}$
  - **Power spectrum** $P(\vec{k}) = \frac{1}{(2\pi)^{3/2}} \int |\vec{v}(\vec{k})|^2 e^{i\vec{k}\vec{r}} d^3\vec{r}$
    - Kolmogorov: $P(\vec{k}) = P(k) \propto k^{-11/3}$
  - **Energy spectrum**
    - Power per dk in Fourier space: $E(k) = 4\pi k^2 P(k)$
    - Kolmogorov: $E(k) \propto k^{-5/3}$ **= Kolmogorov spectrum**
  - Measures the power in a velocity field as function of the spatial wavenumber

In Fourier space

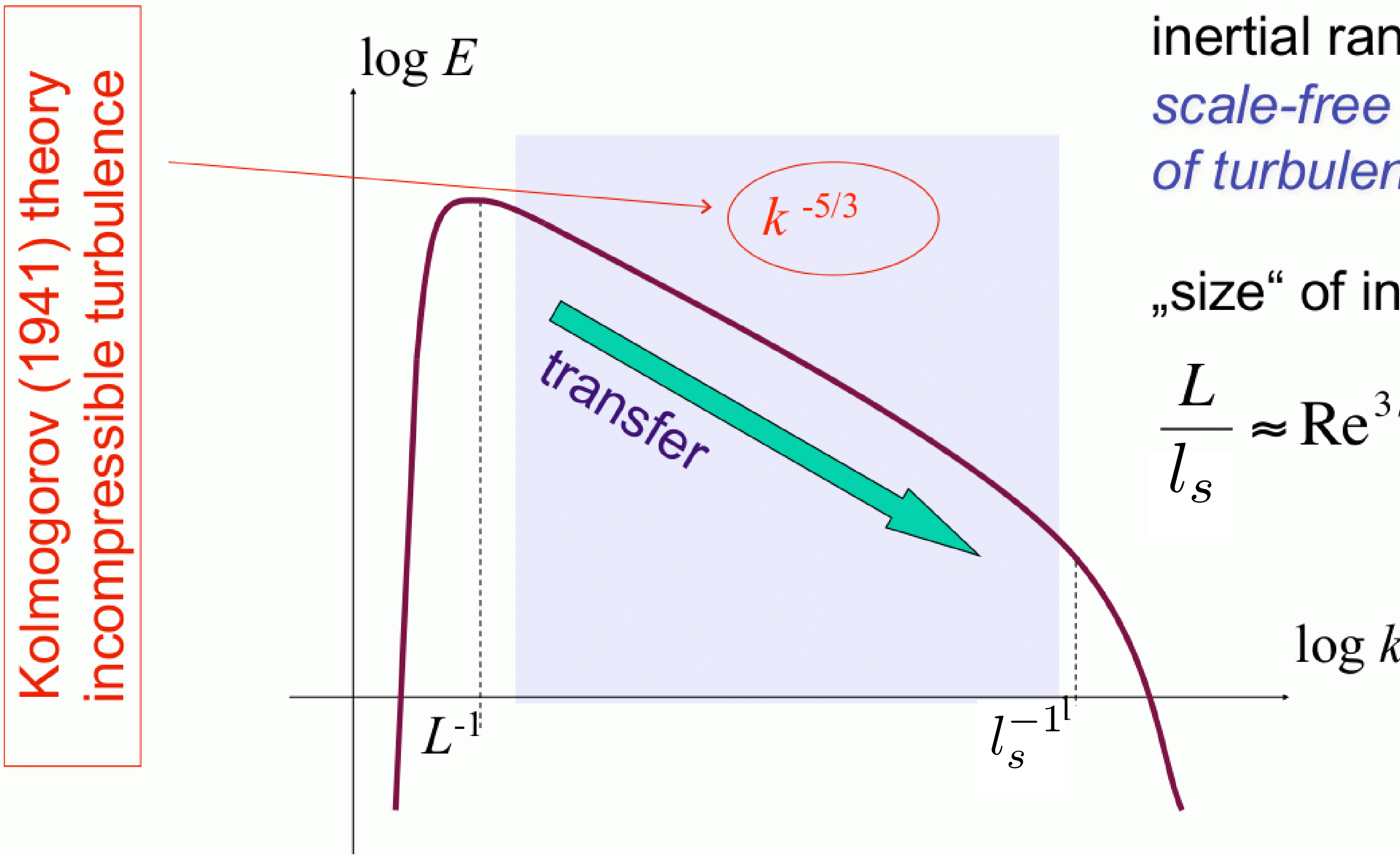

energy
input
scale

energy
dissipation
scale

inertial range:
scale-free behavior of turbulence

„size" of inertial range:

$$\frac{L}{l_s} \approx \mathrm{Re}^{3/4}$$

from R. Klessen (2012)

Turbulence observations

Kolmogorov spectrum

- **Established over wide range of scale**
  - Exponent: -11/3 = -3.67

But: Kolmogorov should only hold for incompressible turbulence
(no density fluctuations considered)

Armstrong, Ricket & Spangler (1995)

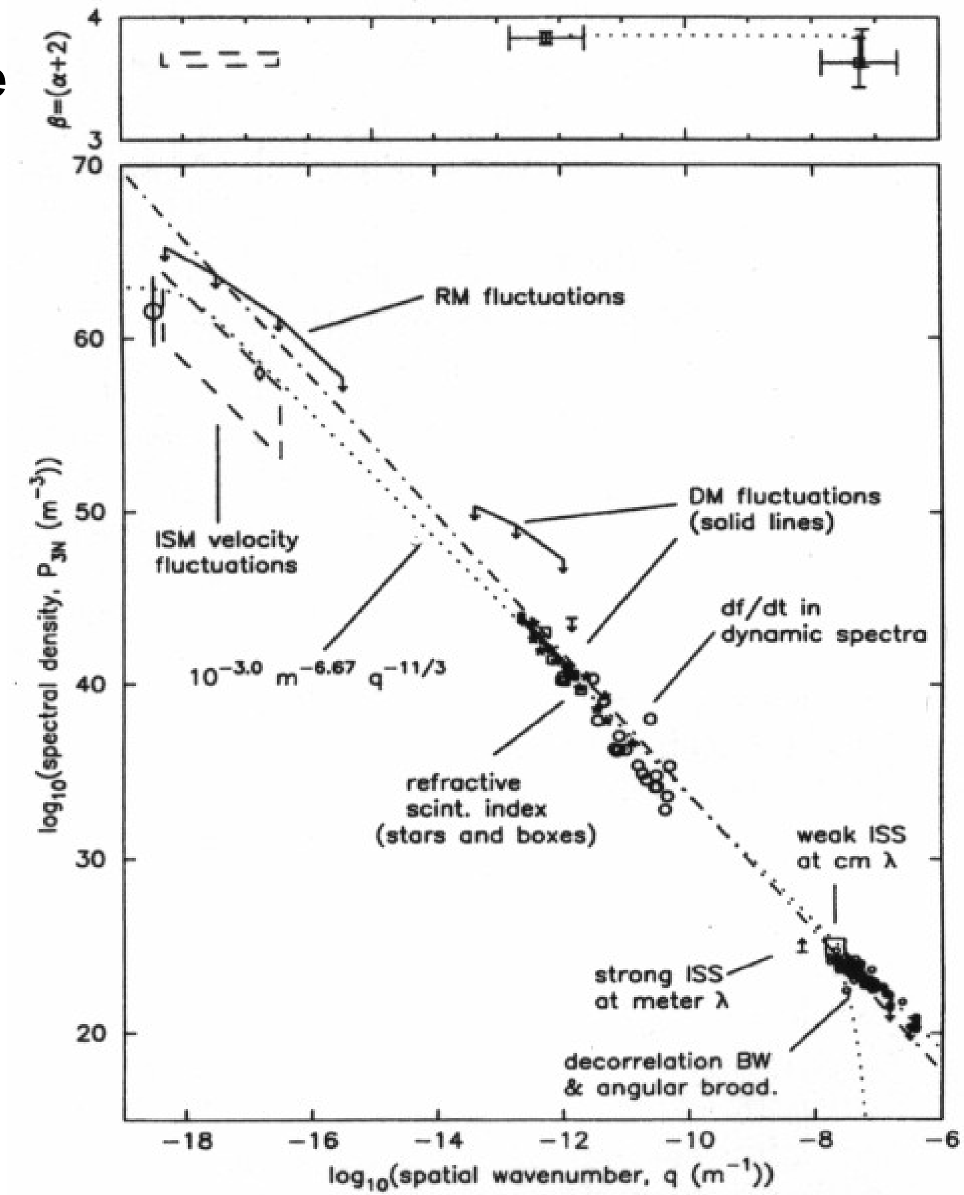

Burgers' turbulence

- **Shocks**
  - Velocity profile:

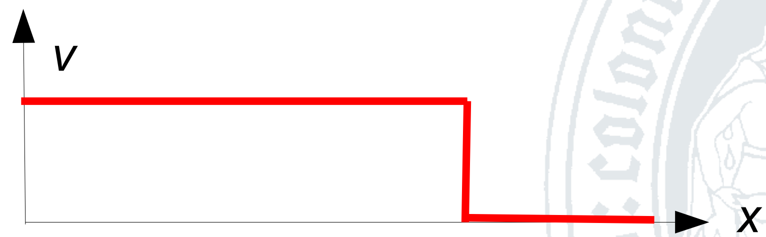

  - **Power spectrum** $$P(\vec{k}) = \frac{1}{(2\pi)^{3/2}} \int |\vec{v}(\vec{k})|^2 e^{i\vec{k}\vec{r}} d^3\vec{r}$$
    $$= \frac{1}{(2\pi)^{3/2}} \int \Theta(x) e^{i\vec{k}\vec{r}} d^3\vec{r}$$
    $$\propto k^{-4}$$
  - **Energy spectrum** $E(k) \propto k^{-2}$
  - Superposition of many shocks in many directions
    - Fourier transform is linear → No change: $E(k) \propto k^{-2}$
    - Burgers' turbulence

Burgers' turbulence

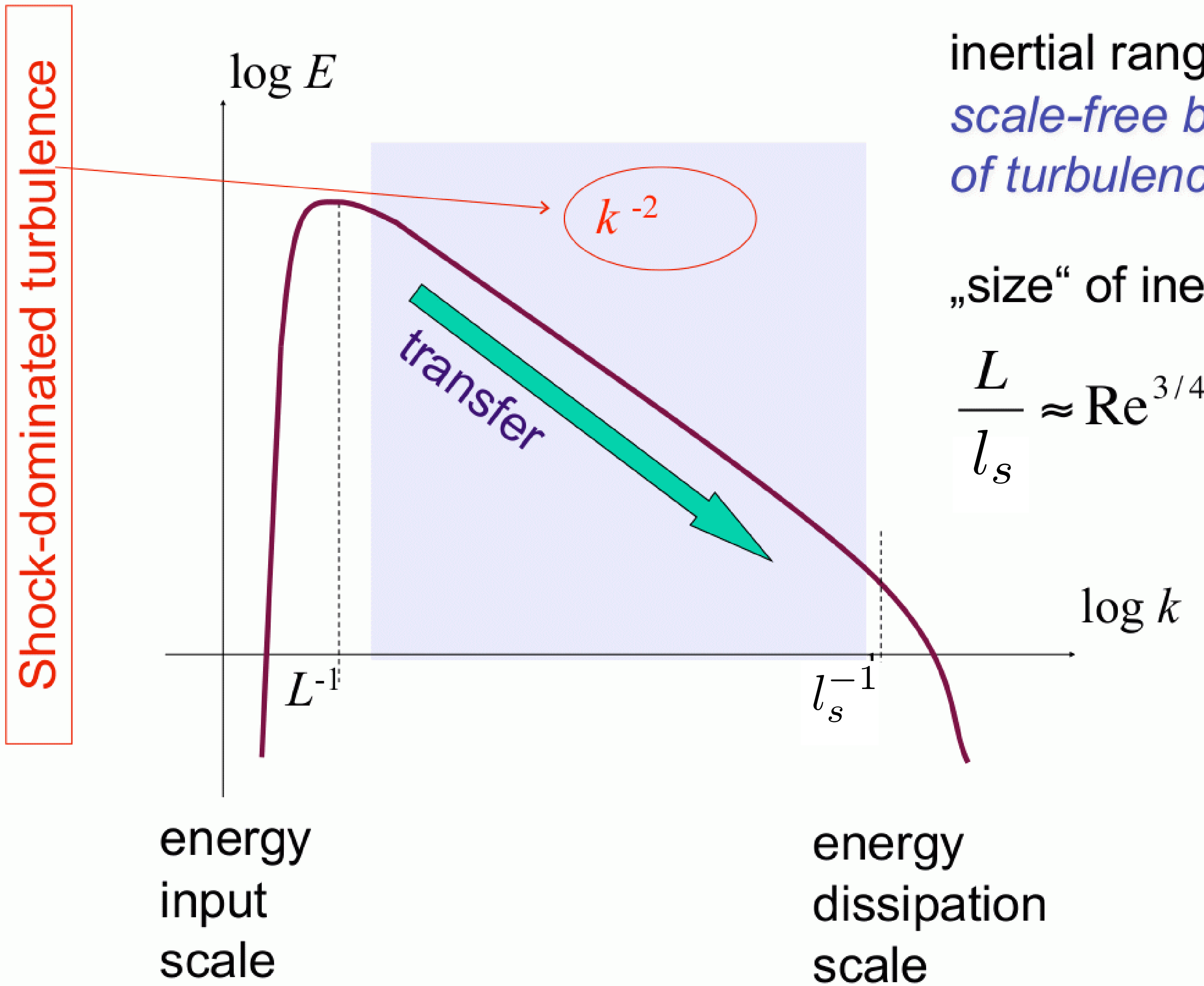

inertial range:
scale-free behavior of turbulence

„size" of inertial range:

$$\frac{L}{l_s} \approx \mathrm{Re}^{3/4}$$

from R. Klessen (2012)

General results

Compressible vs. incompressible turbulence:

- Completely different physics, but only small change on observable spectrum:
  - Kolmogorov: $v(l) \propto l^{1/3}$ $E(k) \propto k^{-5/3}$
  - Burger's: $v(l) \propto l^{1/2}$ $E(k) \propto k^{-2}$
- **Problem:** 3-D velocity measurement from observational data far from trivial

Observations

- Chaotic nature of turbulent field does not allow to identify individual eddies.
  → Measure statistics

- **Statistics of velocity dispersions in clouds: Size-linewidth relation**
  - Larson (1981):

    $$\sigma(\mathrm{km\,s^{-1}}) = 1.10\, L\,(\mathrm{pc})^{0.38}$$

  - Compare Kolmogorov:

    $$\sigma \propto L^{0.33}$$

→ Somewhat steeper

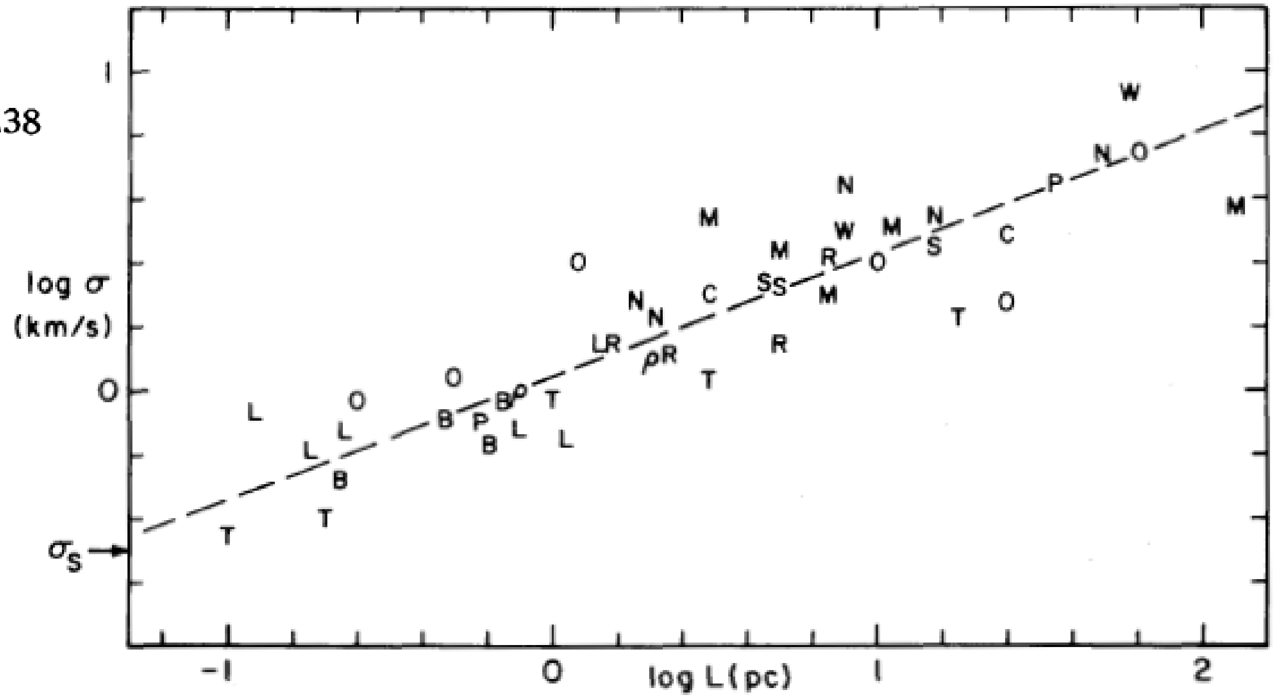

Turbulence observations

Improved velocity measurements

- **Generalized two-point statistics:**
  - Velocity differences as function of spatial separation (Ossenkopf & Mac Low 2002)
  - Applicable to scaling within clouds
  - Virtual beams provide large dynamic range (independently re-invented by Leroy et al. 2015)
  - Result:

$$\Delta v \propto l^{0.5}$$

  - Steeper than Larson (1981)
  - Not consistent with Kolmogorov!

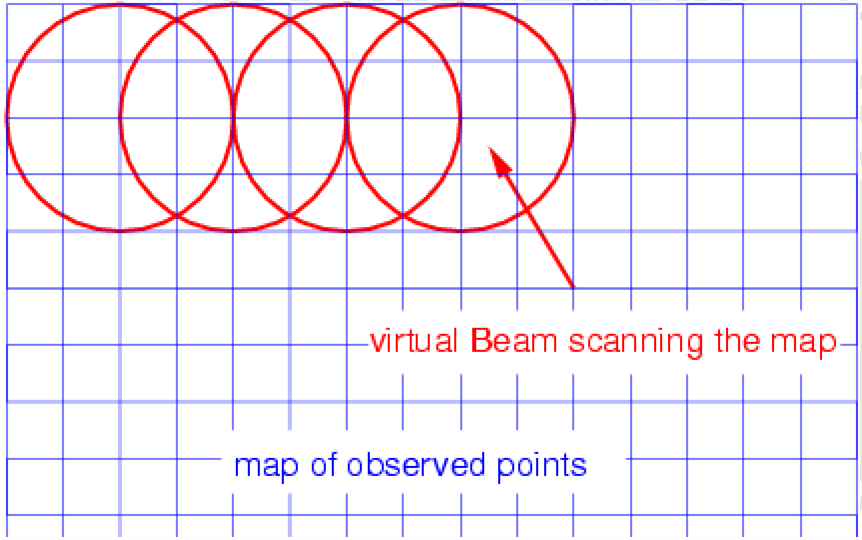

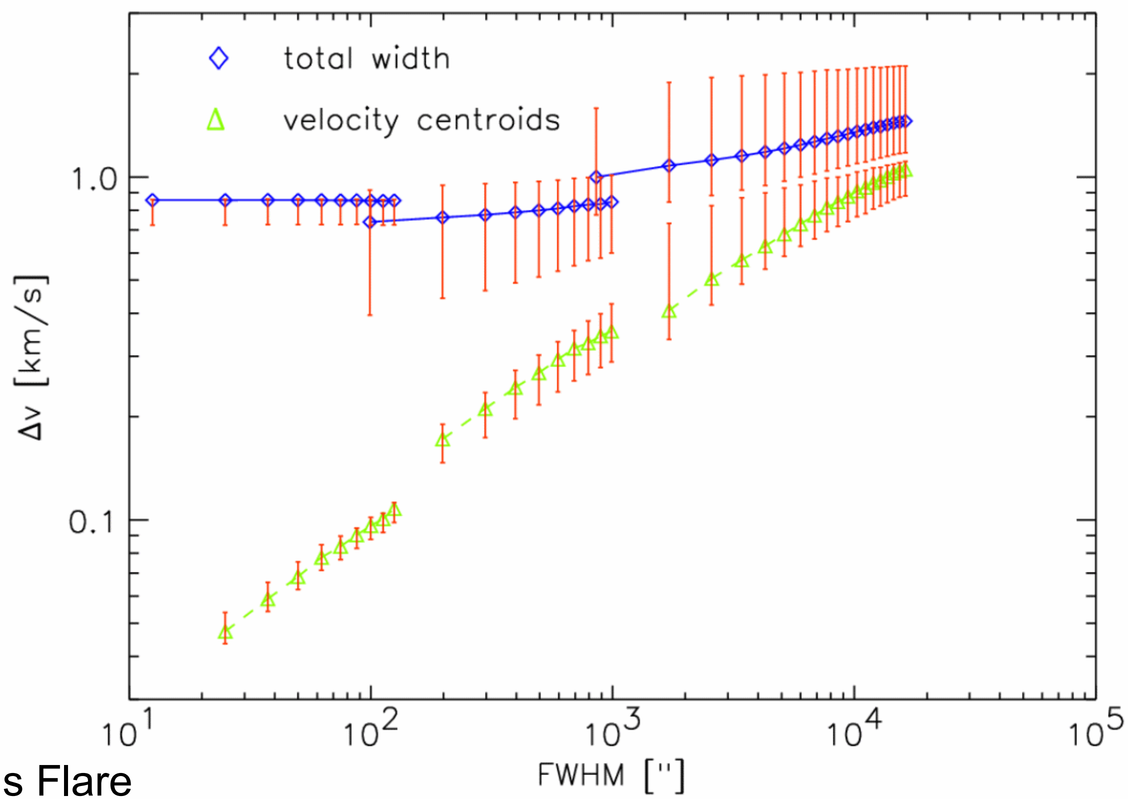

Velocity field in Polaris Flare

More general result

- Density-dependent velocity scaling relations (Heyer 2009)
  - $\Delta v(l) \propto l^{0.5}$ applies for specific column density only
  - Consistent with:
    - Shocks (Burgers' turbulence)
    - Freely collapsing cores
    - Clumps in virial equilibrium

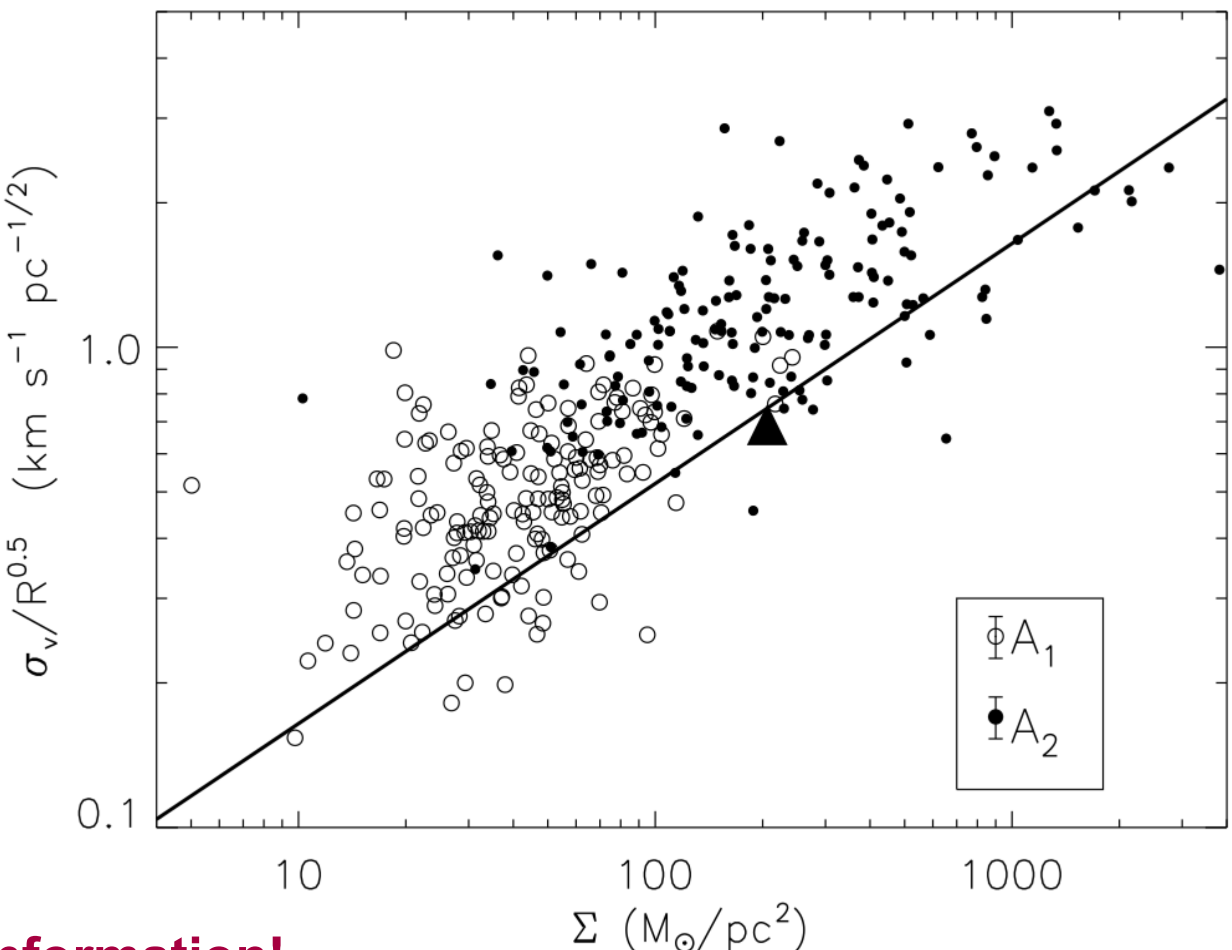

- **Very little discriminating information!**

How to discriminate?

Density structure

- Kolmogorov: incompressible hydrodynamics
  $\rightarrow$ no density structure
- Burger's turbulence: box full of shocks (step function)
  $\rightarrow$ full compressibility

- Actual density structure
  - Log-normal density distribution

$$p(s) = \frac{1}{\sqrt{2\pi}\sigma_s} \exp\left(\frac{[s-s_0]^2}{2\sigma_s^2}\right)$$

with $s = \ln\left(\frac{n}{\langle n \rangle}\right)$

- Problem: not directly observable

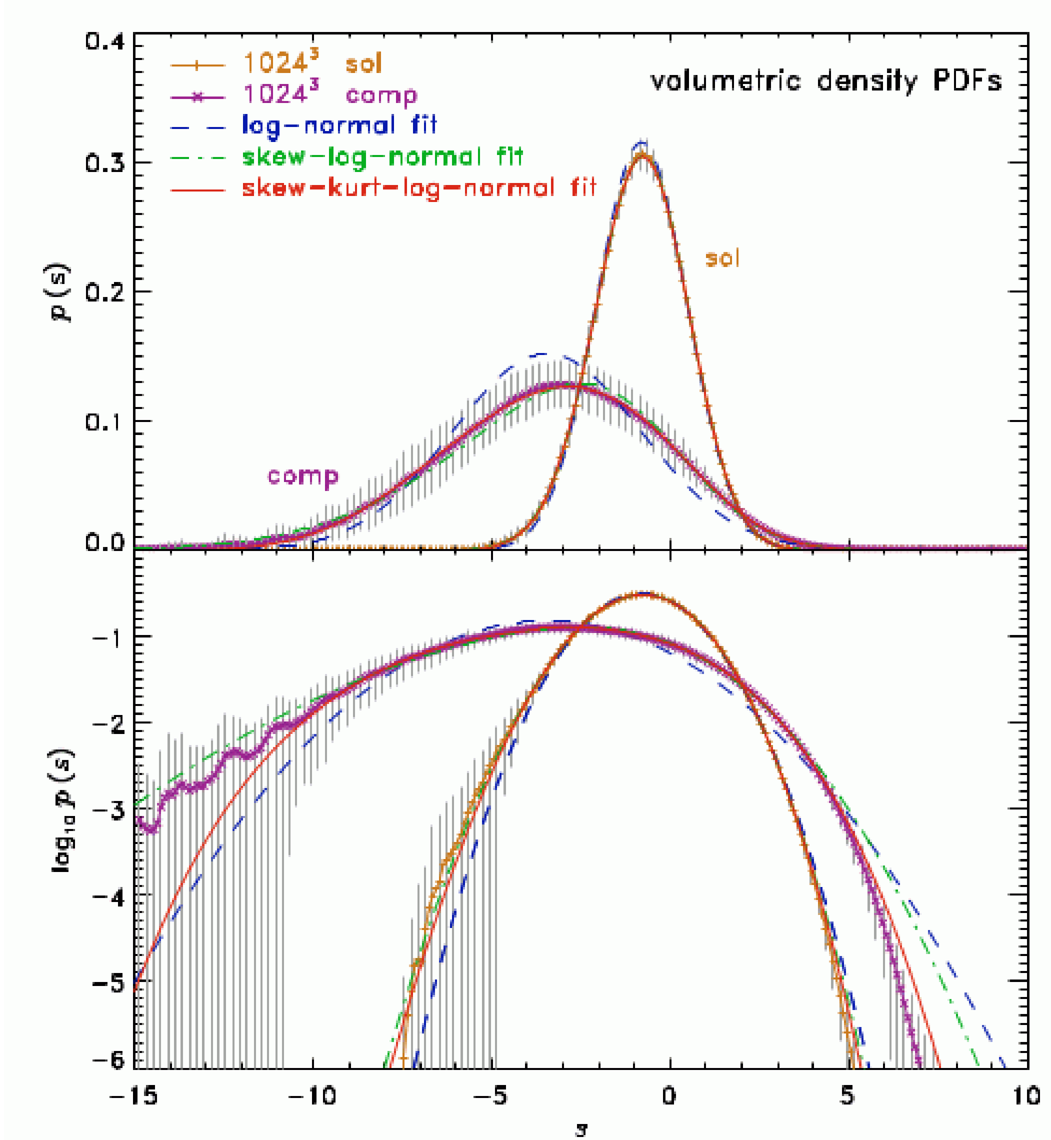

Federrath (2010)

Column densities

Column-density probability distribution functions (PDFs):

- From turbulence simulations (Padoan & Nordlund 1999)

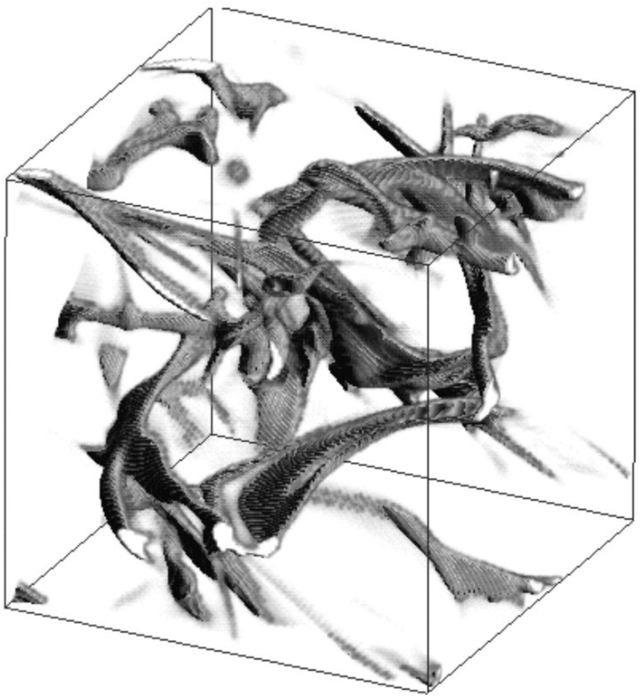

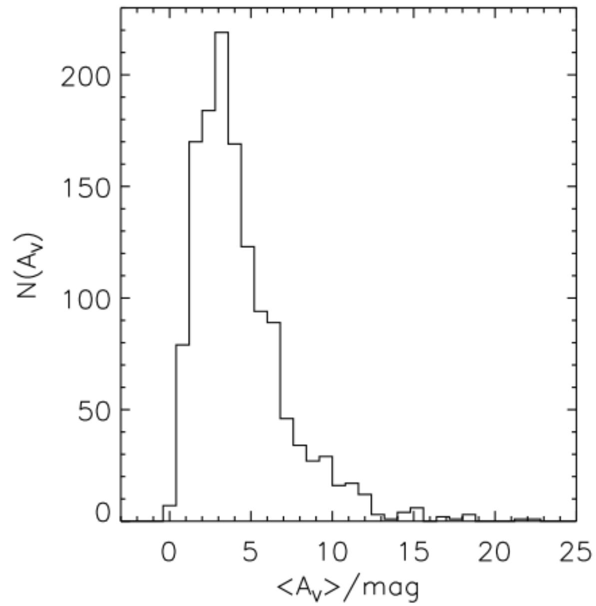

PDF of supersonic model

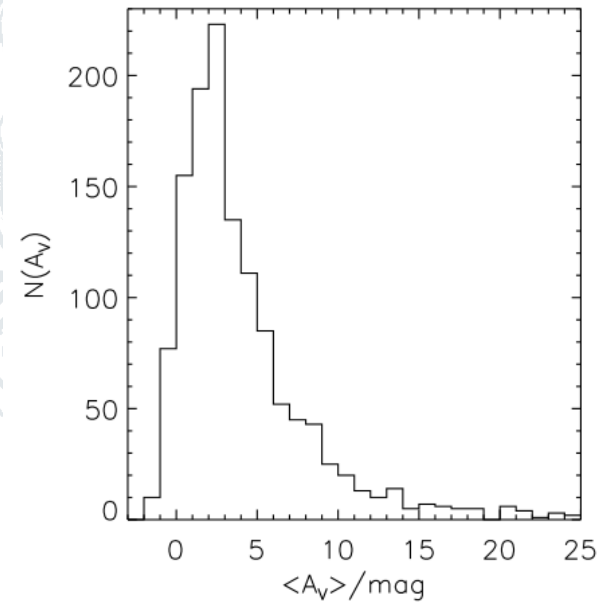

Observed in IC5146 (Lada et al. 1994)

– For logarithm of column densities: $\eta = \ln\left(\frac{N}{N_{\mathrm{peak}}}\right)$

→ Gaussian shape: $p_\eta(\eta) = \frac{1}{\sqrt{2\pi}\sigma_\eta} \exp\left(-\frac{\eta^2}{2\sigma_\eta^2}\right)$ → **log-normal**

Probability distribution functions of column densities

Log-normal PDFs of turbulent media:

- PDF width σ_η determined by Mach number (Passot & Vazquez-Semadeni 1998)

$$\sigma_\eta^2 = A \times \ln\left(1 + b^2 \mathcal{M}_\mathrm{s}^2\right)$$

- b = parameter for the geometry of driving
  - $b = 1/3$ for solenoidal driving (in vortices)
  - $b = 1$ for compressive driving (in shocks)
  - $b = 5/9$ for random mix

  (Federrath & Brunt 2014)

- **Theoretical background still debated**

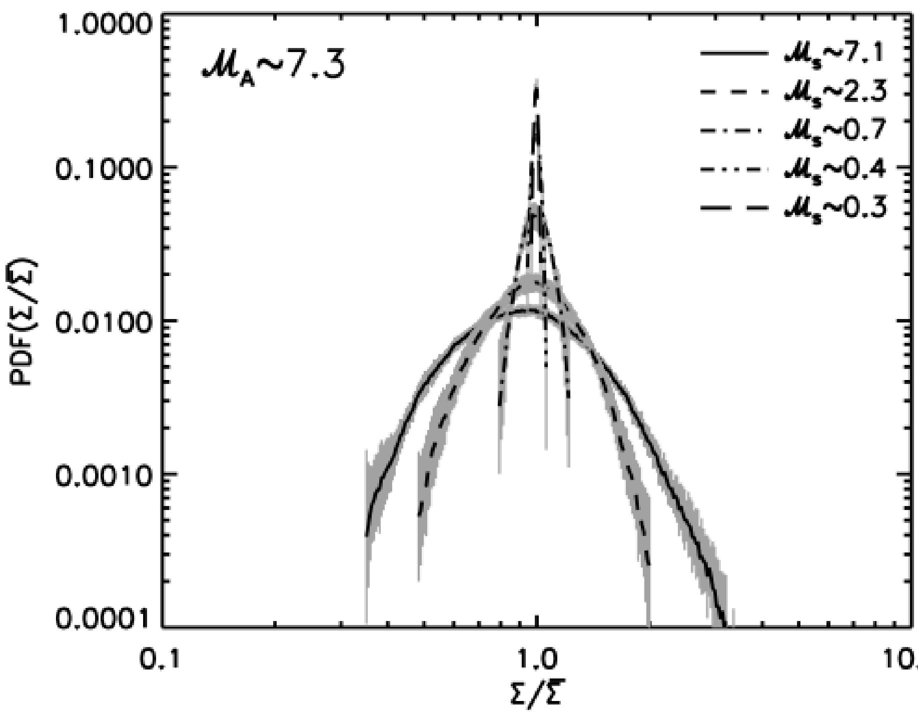

Column-density PDFs from isothermal simulations with different sonic Mach numbers (Kowal et al. 2007)

- Small asymmetries depending on the magnetic field impact

Turbulent column density PDFs

Phase transitions:

- Different phases: – different equation of state
  – different Mach numbers → double-peak PDFs

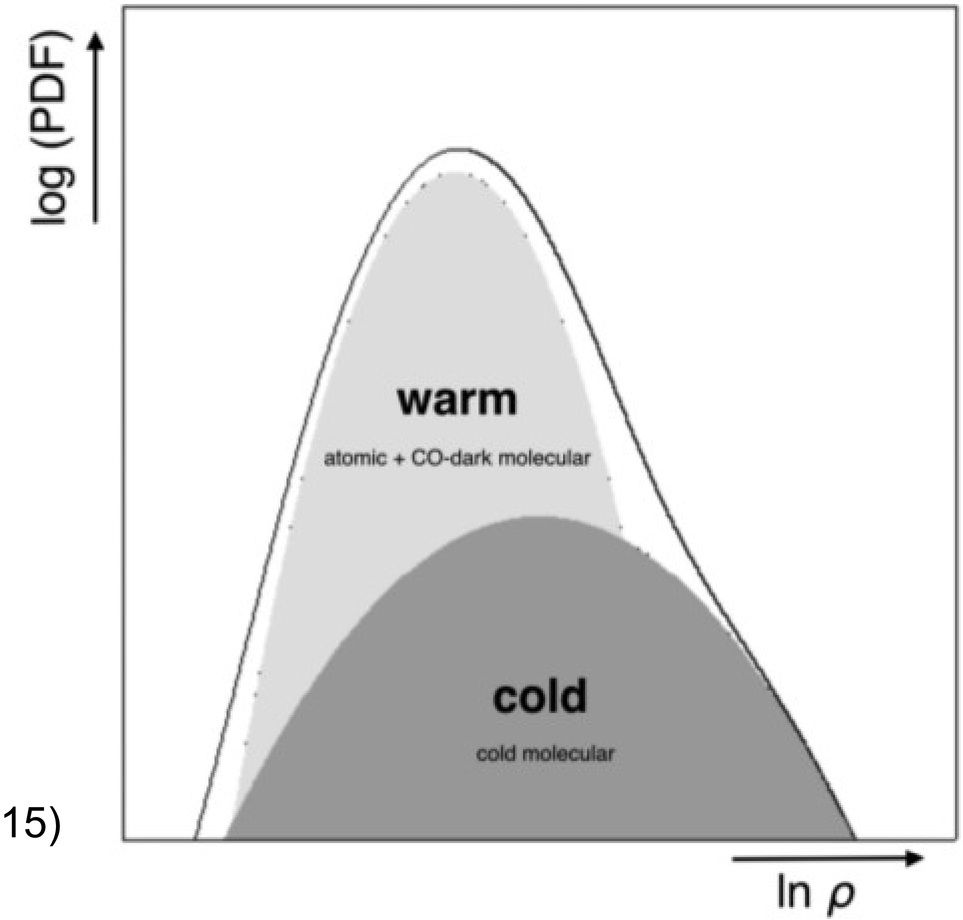

Brunt (2015)

– Important transition for molecular clouds: HI – H_2

Phase transitions

Observation: Draco

- Intermediate-velocity cloud, possible template for colliding flow
- Transition of HI → H_2 and C^+ → C → CO
- Weak CO detection (Stark et al. 1997)

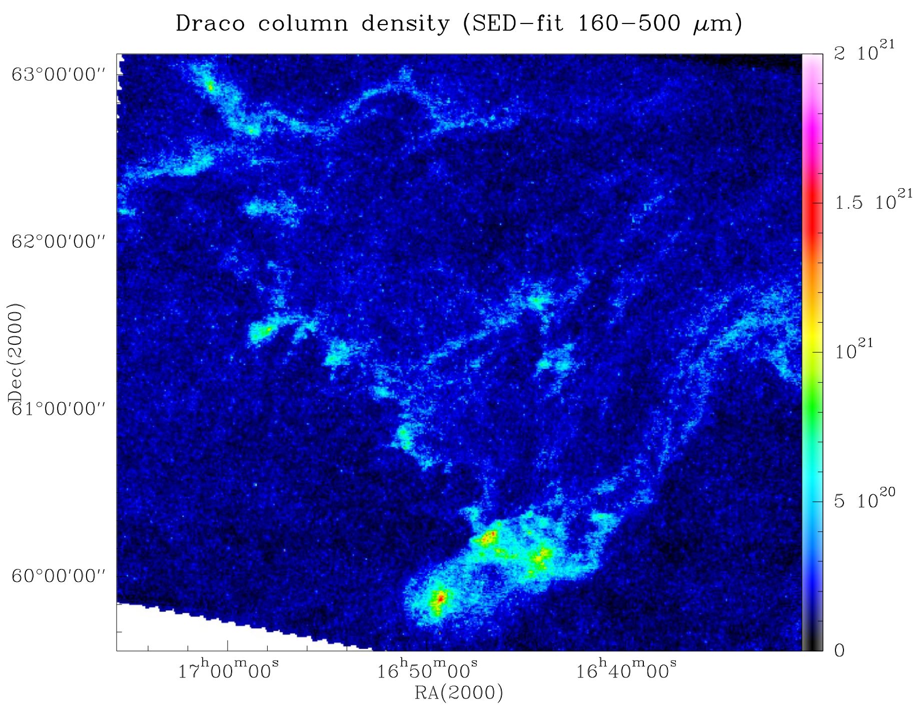

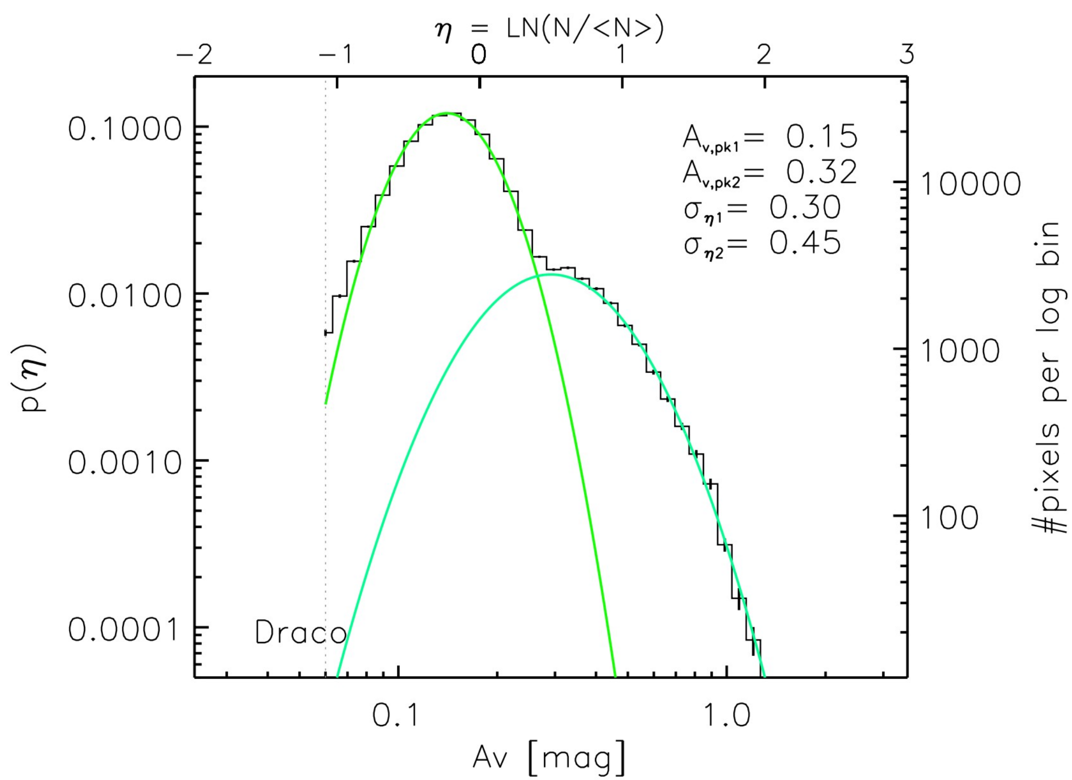

Total column density: Schneider et al. (subm.)

– Two peaks, separation at $A_V \approx 0.3$ → assignment to phases

Gravity

Power law tails in PDFs:

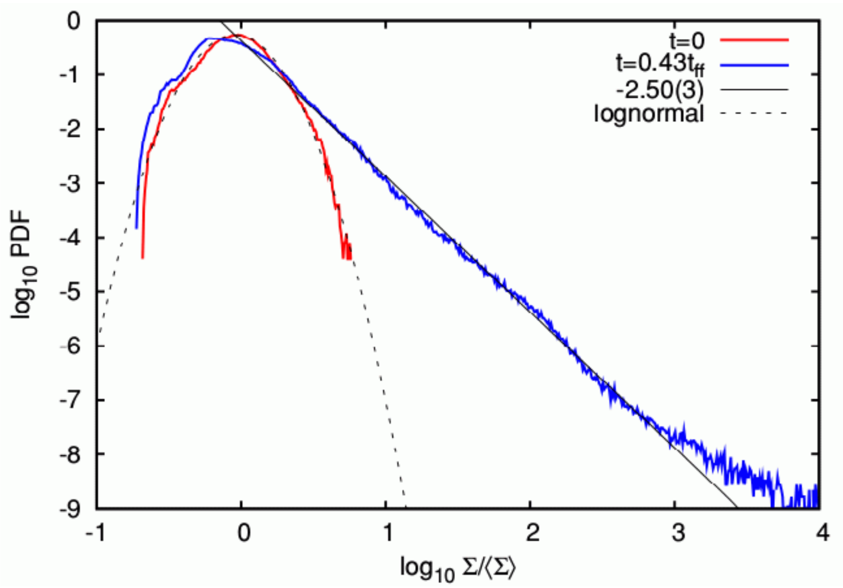

PDF of collapsing model (Kritsuk et al. 2011)

- **Self-gravity unavoidably creates power-law tails**

Ballesteros-Paredes et al. 2011; Kritsuk et al. 2011; Girichidis et al. 2011, 2014; Federrath & Klessen (2013); Froebrich & Rowles 2010; Myers 2015; Toci & Galli 2015, Passot & Vazquez-Semadeni 1998; Kainulainen et al. 2009, 2011; Tremblin et al. 2013, 2014, ...

- Power-law tail: $p_\eta(\eta) = \left(\frac{N}{N_{\rm peak}}\right)^{-s}$
  - Exponent depends on density profile: $n(r) \propto r^{-\alpha}$
    - $s = 2/(\alpha - 1)$ for spherical symmetry (cores)
    - $s = 1/(\alpha - 1)$ for cylindrical symmetry (filaments)

Observations

PDF in Orion B (Schneider et al. 2013)

→ Compare log-normal part and power-law tail

→ Key to quantify relative influence of turbulence and gravity

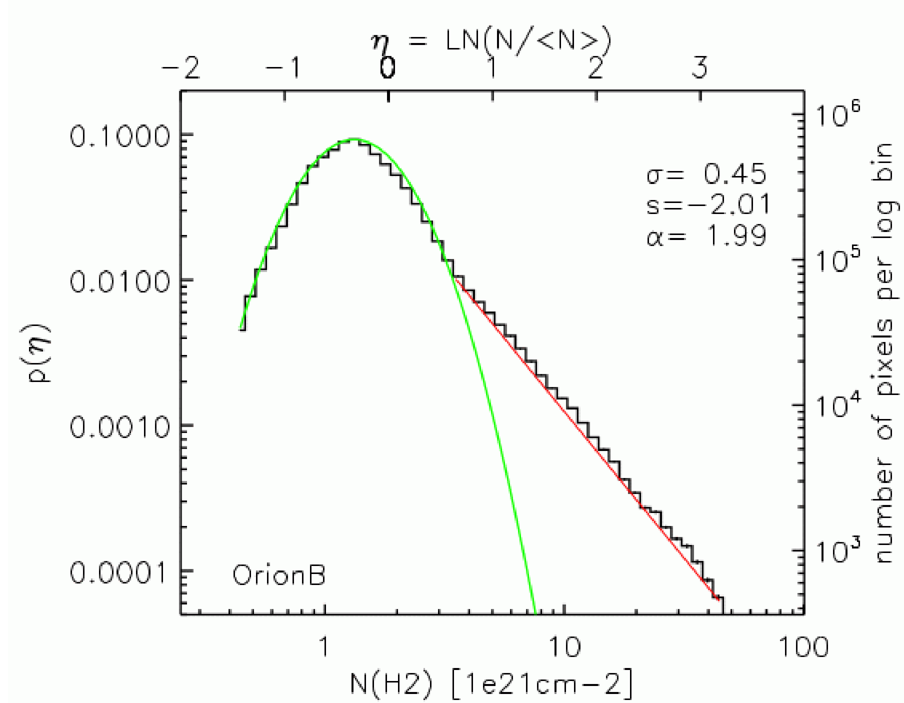

– But: very careful data analysis needed to distinguish different cases

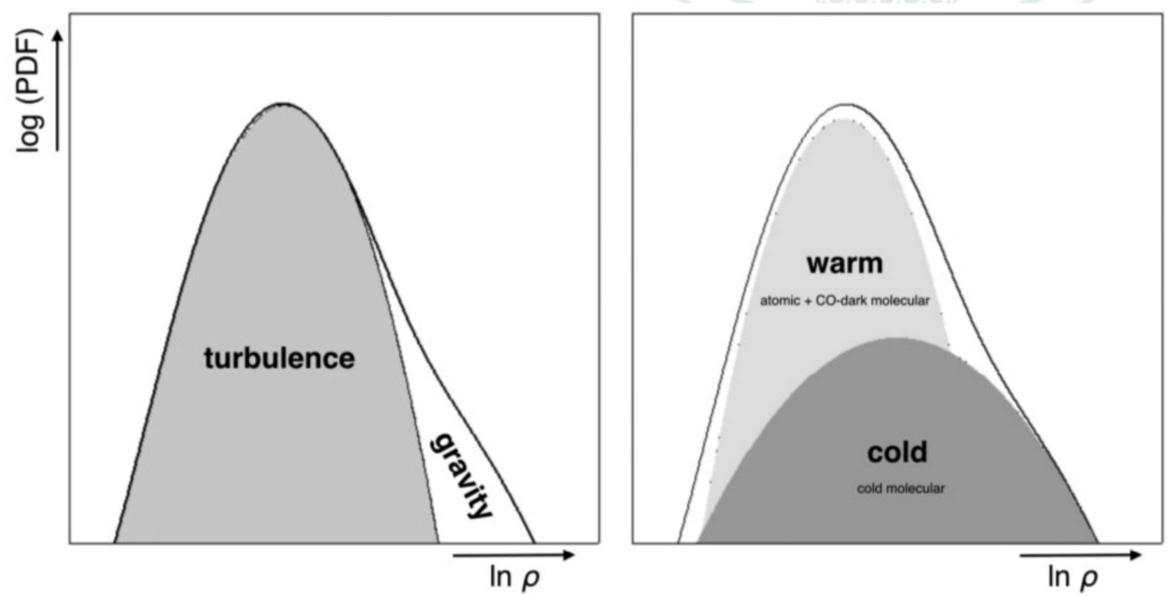

Brunt (2015)

Problems

Line-of-sight contamination:

- IRDC G28.37+0.07:
  - Analysis of extinction and Herschel column density maps
  - Kainulainen & Tan (2013), Lim et al. (2016):
    - purely log-normal
  - Schneider et al. (2015):
    - only power law tail
  - **from the same data!**

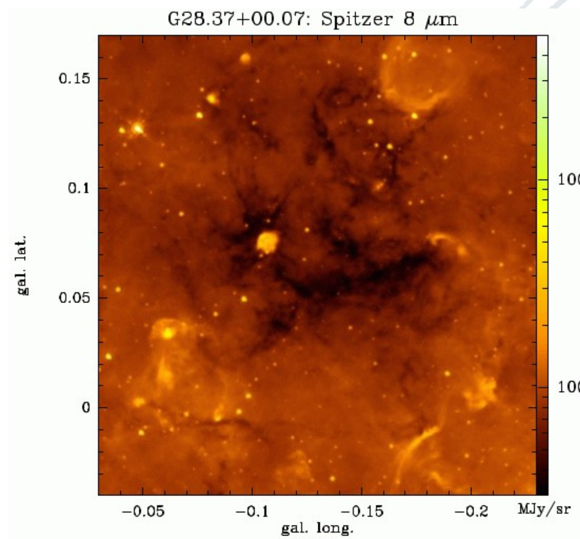

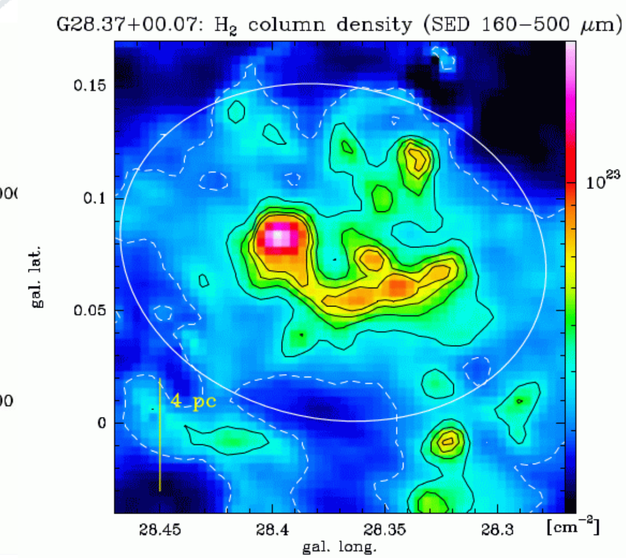

IRAC 8µm

Herschel column density

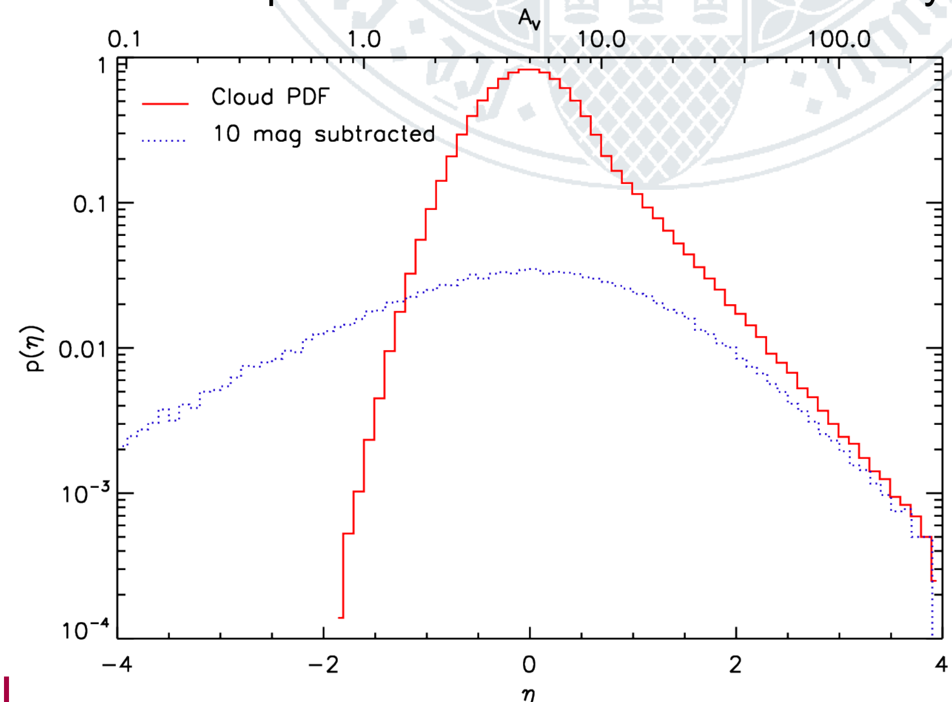

Ossenkopf-Okada et al. (2016)

Explanation:

- Different level of assumed line-of-sight (LOS) contamination
- LOS “overcorrection” creates PDF that seems log-normal, but has power-law tail

Further surprises

- Two power law tails:
  - Common, but not omnipresent in massive GMCs
  - Excess with $\alpha > 2$ must be caused by a process that reduces the flow of mass towards higher densities at $A_V \geq 50$
  - Cause: Unknown so far

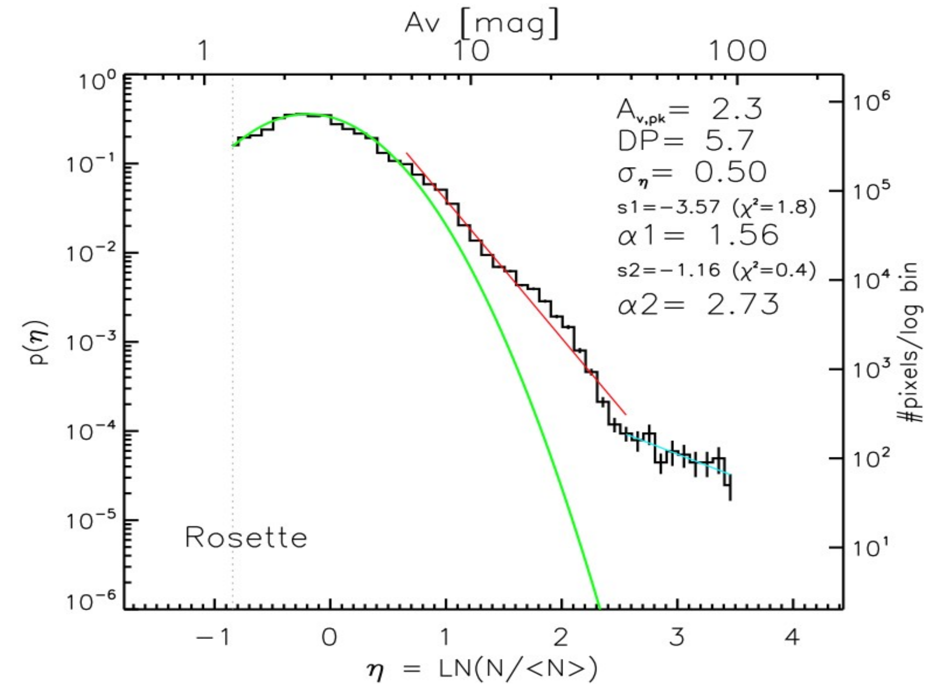

Schneider et al. (2015c)

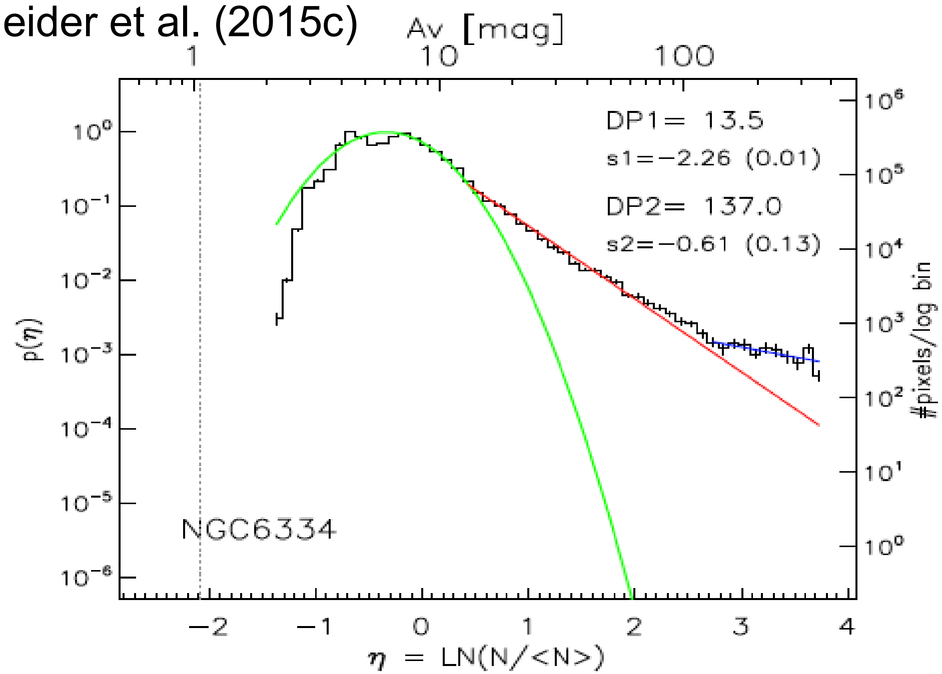

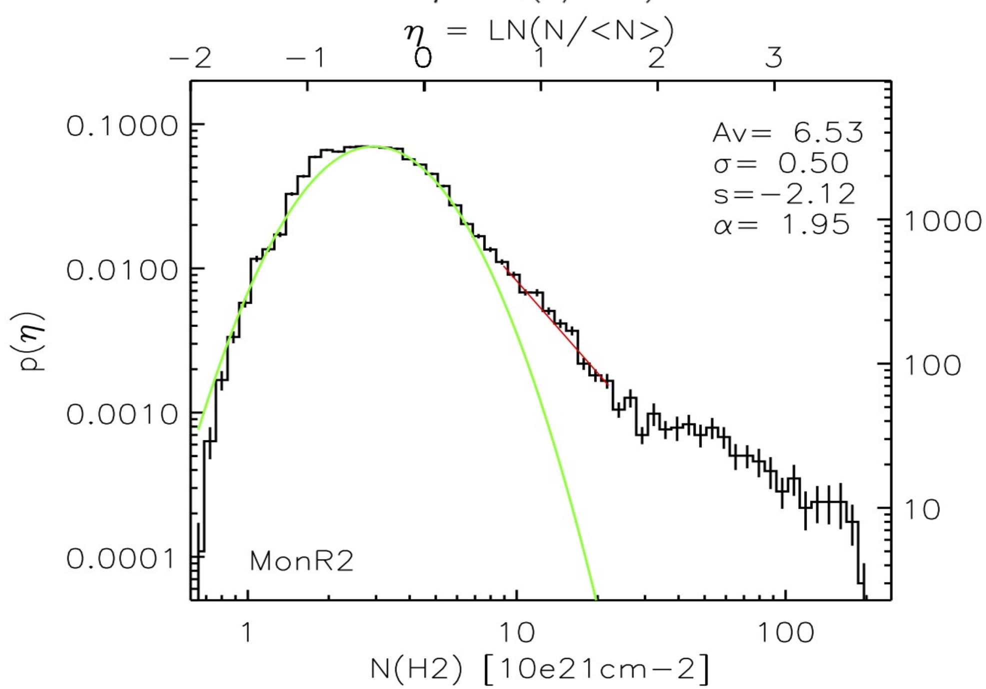

Spatial structure

Turbulence

- **Hierarchical structure**
  - Cascade of motions with different size

    → Look for the hierarchical structure in the spatial scaling

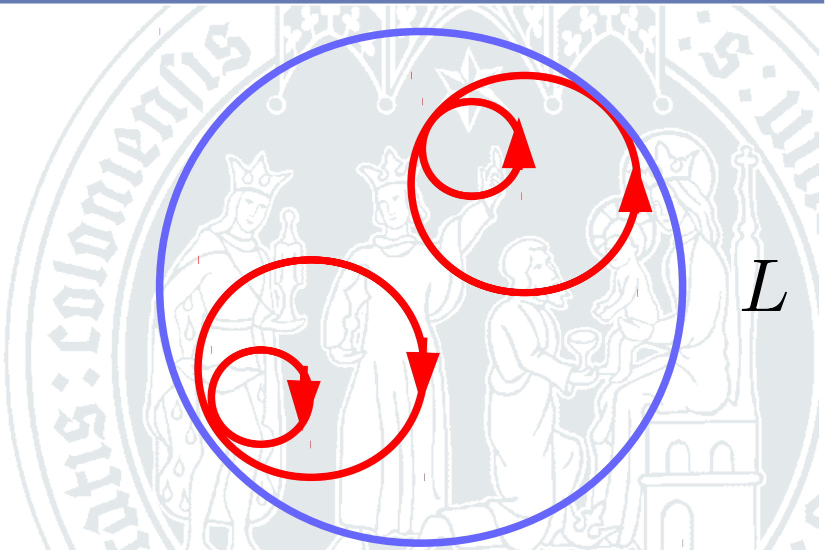

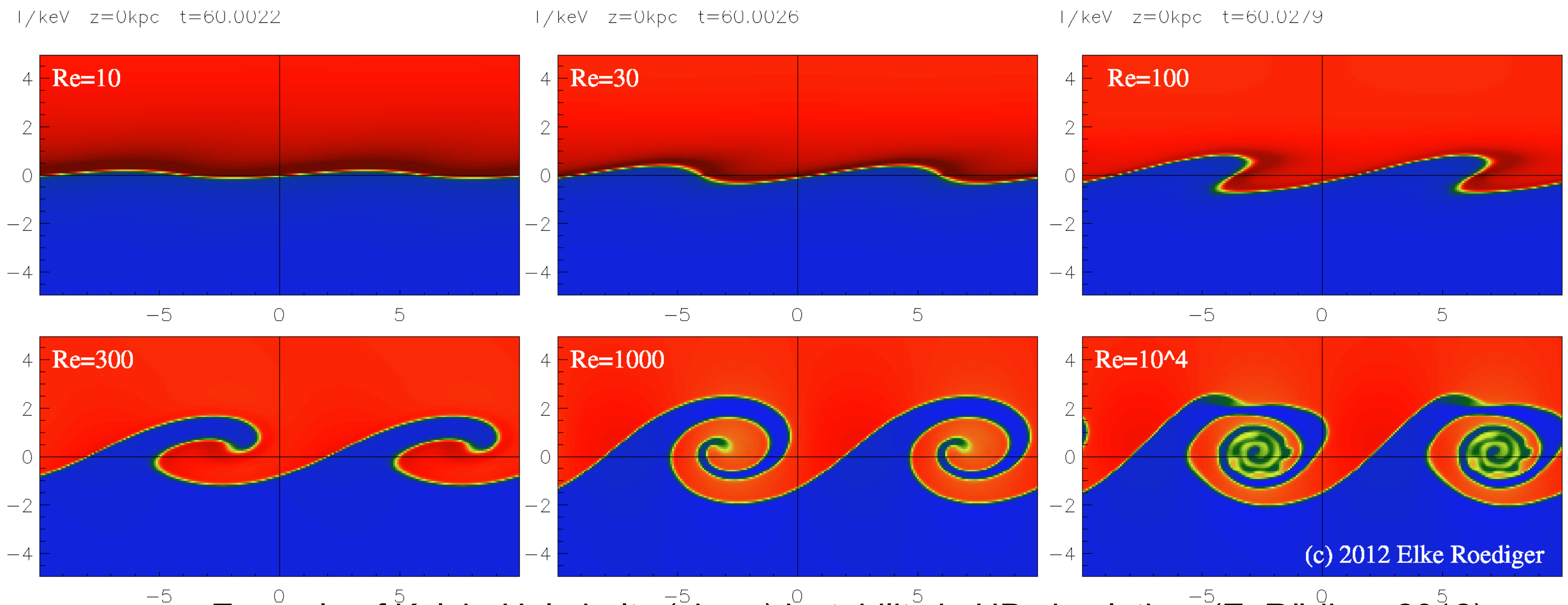

Example of Kelvin-Helmholtz (shear) instability in HD simulation (E. Rödiger 2012)

Turbulent cascade

Self similarity

- **Same type of structures on all scales**
  - Confirmed by observations:

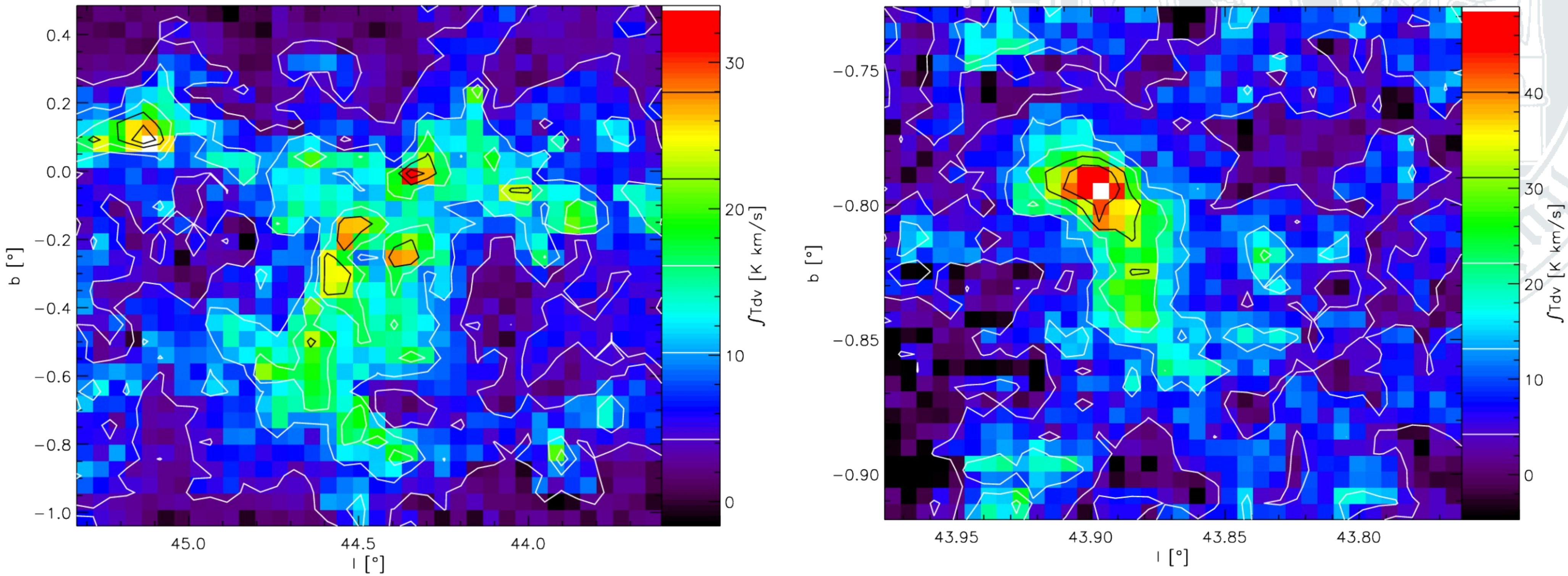

  - Integrated ^{13}CO 1-0 line map from the BU-FCRAO survey of the Galactic Ring at different "zoom levels" (Simon et al. 2002)
  - ☞ Self-similar over a large range of scales.

Measure spatial scaling

Power spectrum

Scale invariance results in a power-law power spectrum: $P(k) \propto k^{-\beta}$

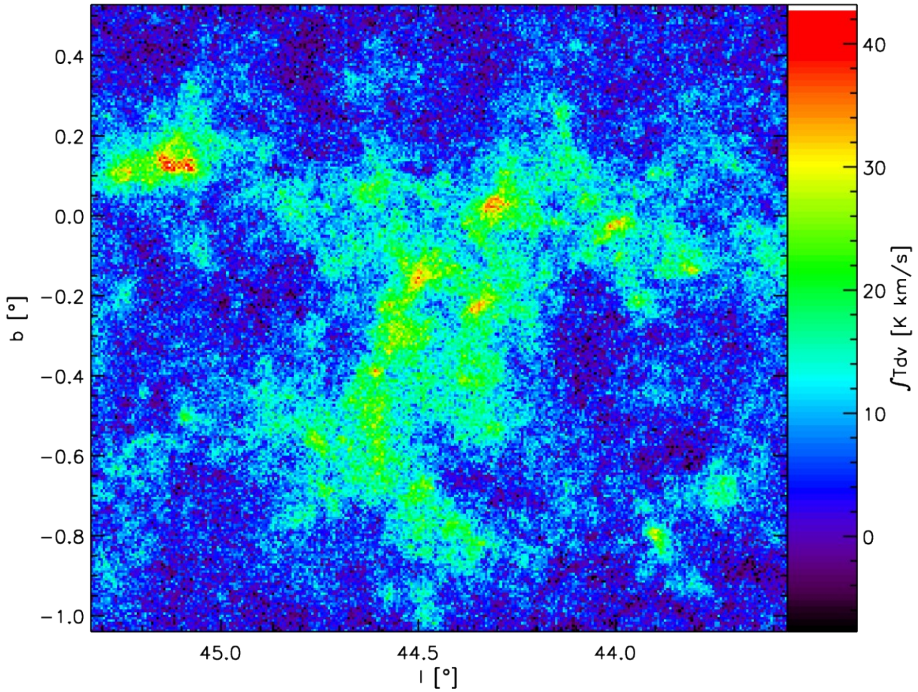

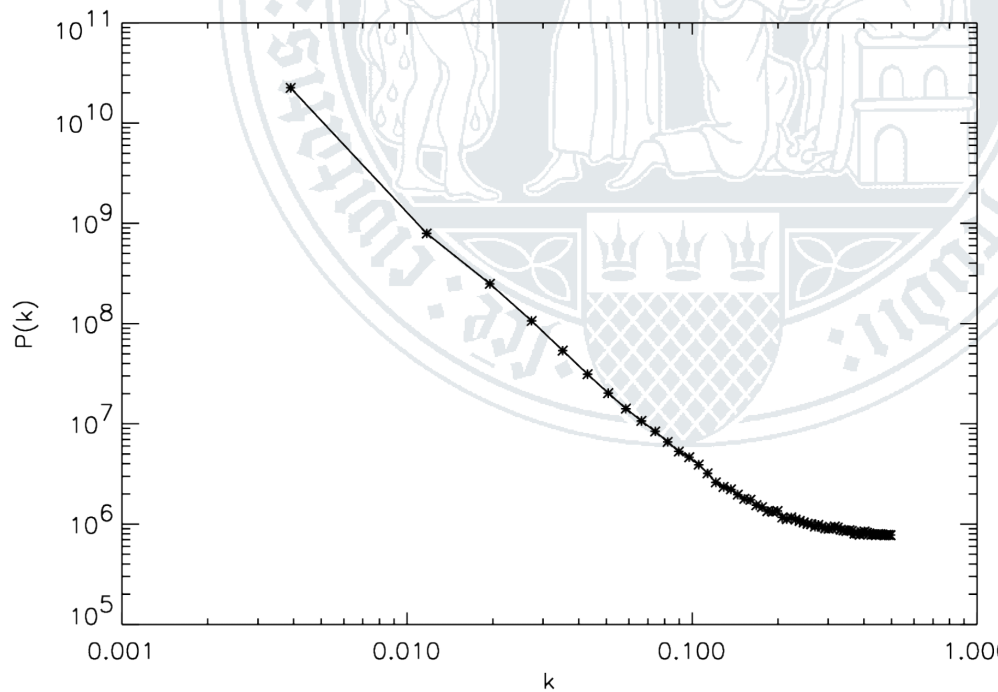

Analysis of G44.5 subfield of ^{13}CO 1-0 line map from BU-FCRAO-GRS

- For rectangular maps, the power spectrum can be easily computed by FFT.

Measure spatial scaling

Δ-variance

Filter map by radially symmetric wavelet $\psi_l(r)$

- characteristic length scale *l*
- Measure variance in convolved image as function of the filter size *l*

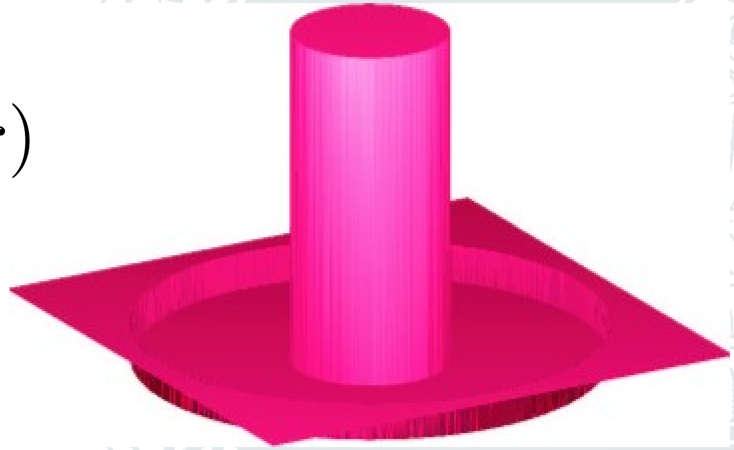

- **Main advantage**
  - Δ-variance can measure the spatial scaling of irregular maps and maps with variable noise.
  - In the practical application the Δ-variance is much more robust than the power spectrum, but provides the same type of information.

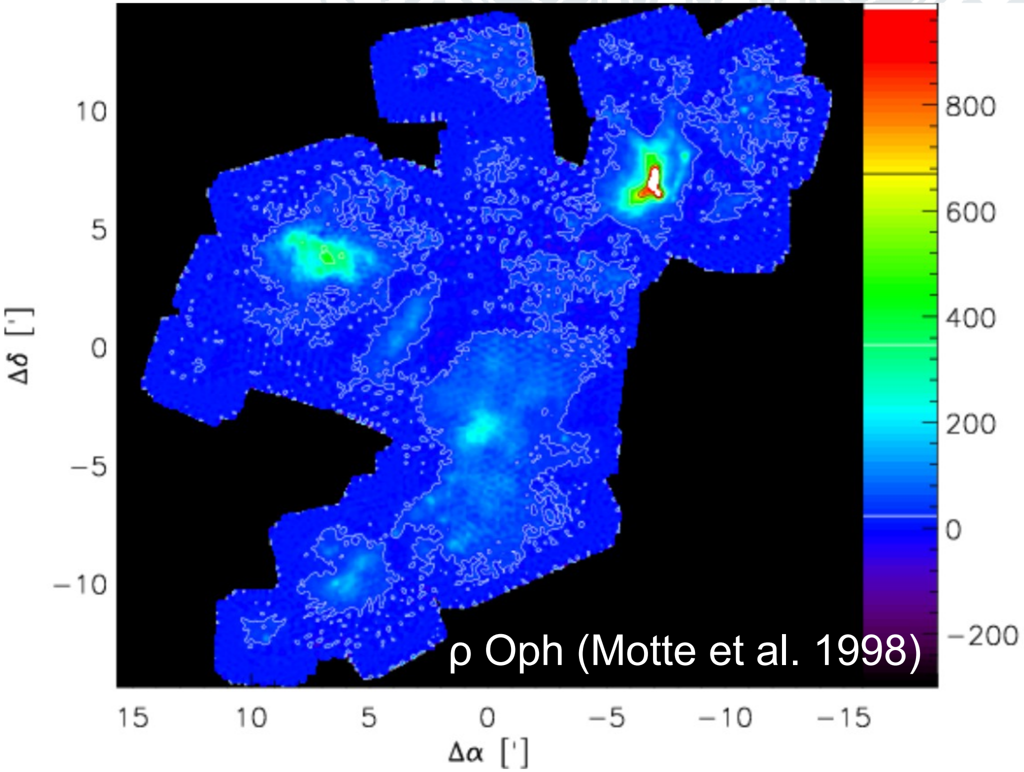

Δ-variance

Power-law power spectrum gives power-law Δ-variance: $\sigma_\Delta^2(l) \propto l^\alpha$

- Spectral index related to the power spectral index by $\alpha = \beta - 2$.

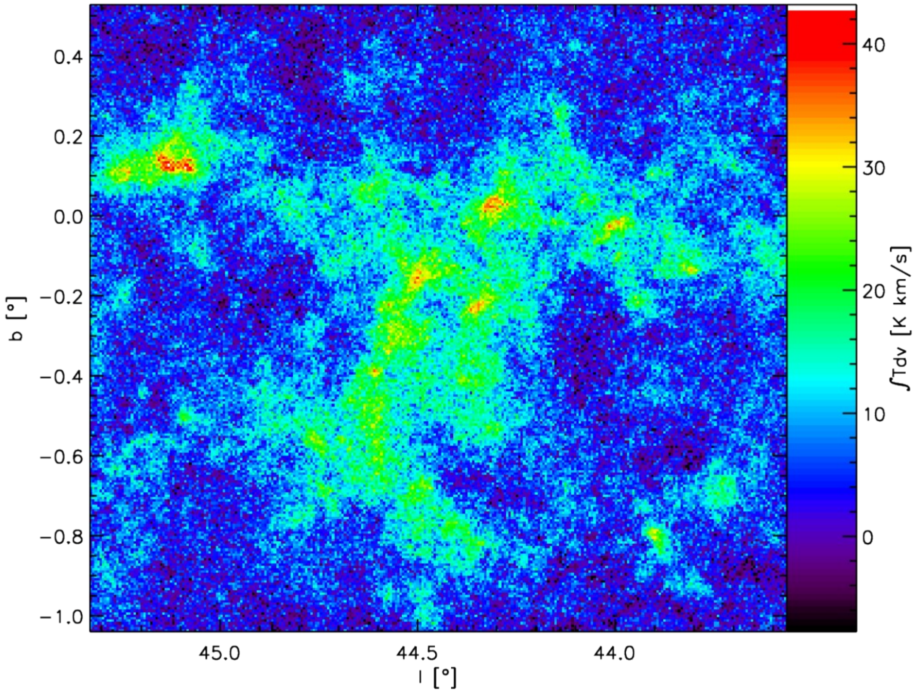

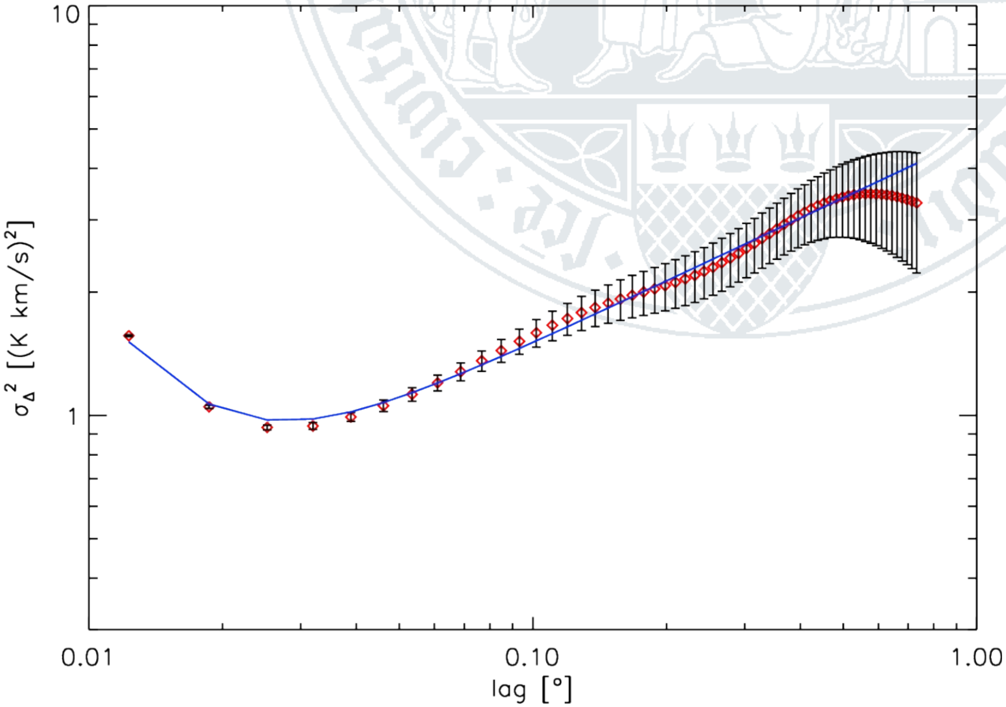

Analysis of G44.5 subfield of ^{13}CO 1-0 line map from BU-FCRAO-GRS

Measure spatial scaling

Turbulence models:

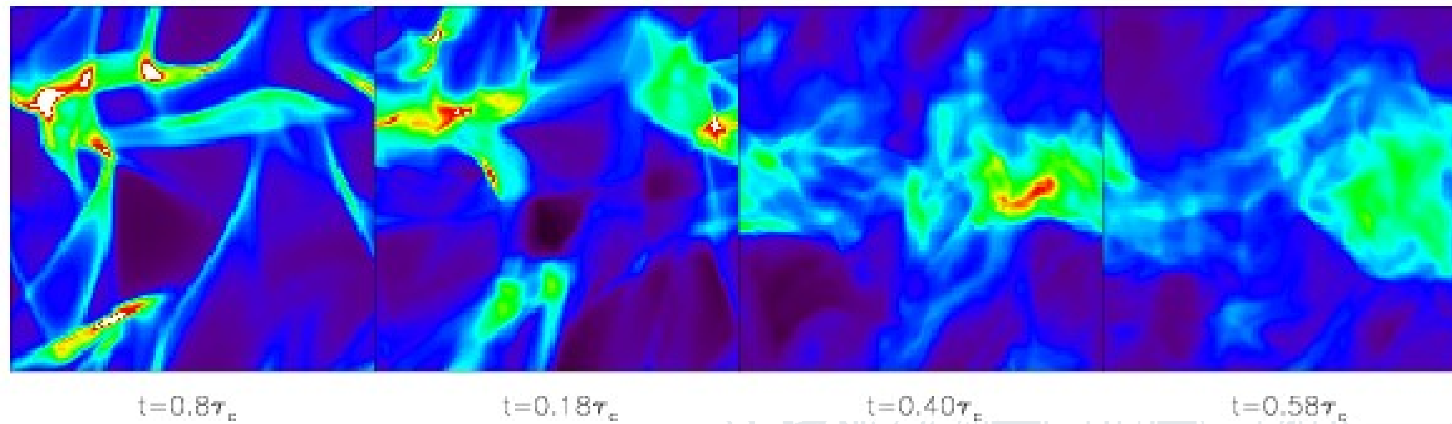

Column density evolution in a HD turbulence simulation (Mac Low et al. 1998)

Resulting Δ-variance spectra with progressing dissipation of energy

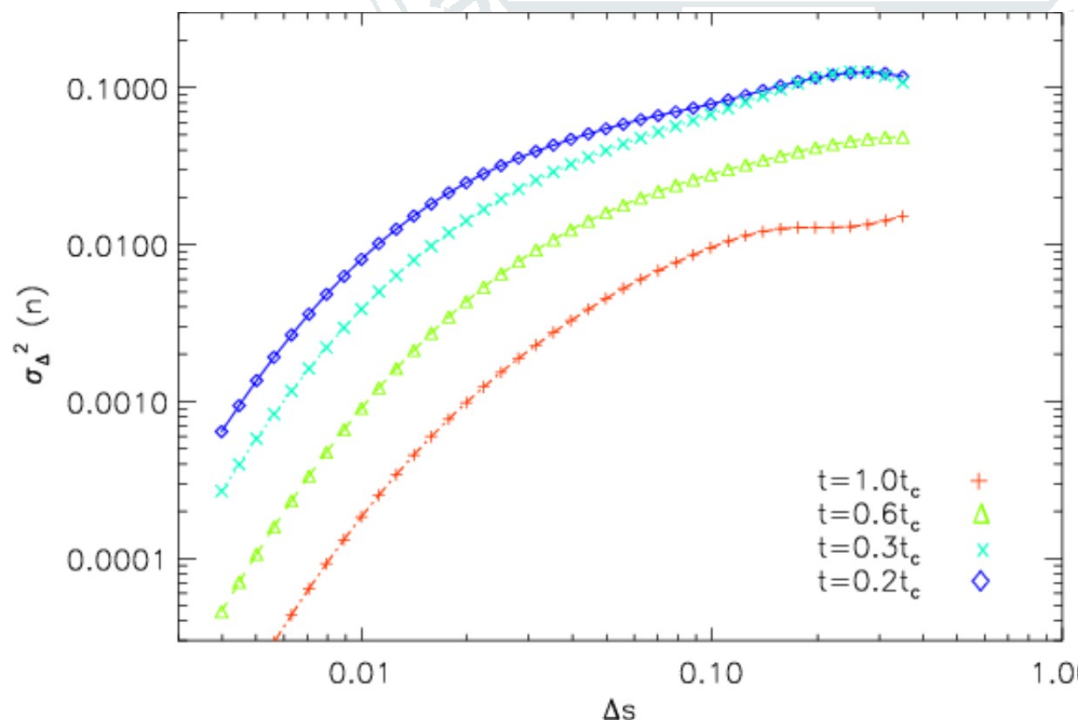

Results:

- Only models driven at large scales reproduce the observed self-similar scaling.
- Different processes reveal themselves by slope changes.

☞ Key to different physical processes is to detect deviations from self-similarity.

Formation

- 3 different processes discussed

Gravity-dominated cloud formation

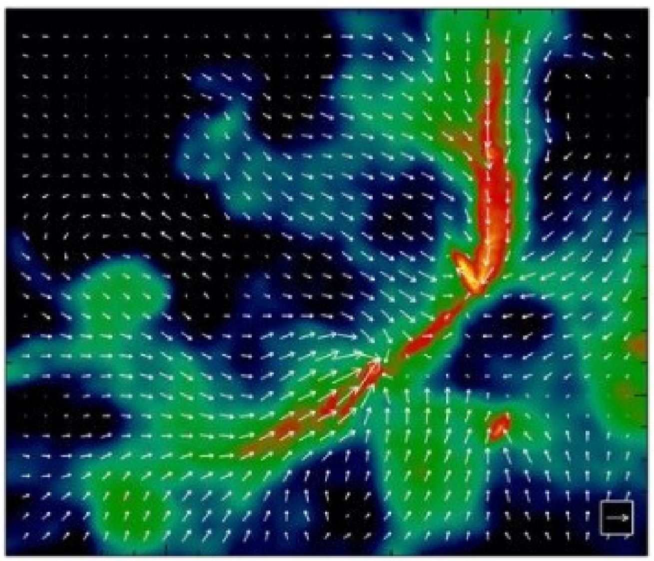

e.g. Gomez & Vazquez-Semadeni (2014)

Turbulent fragmentation

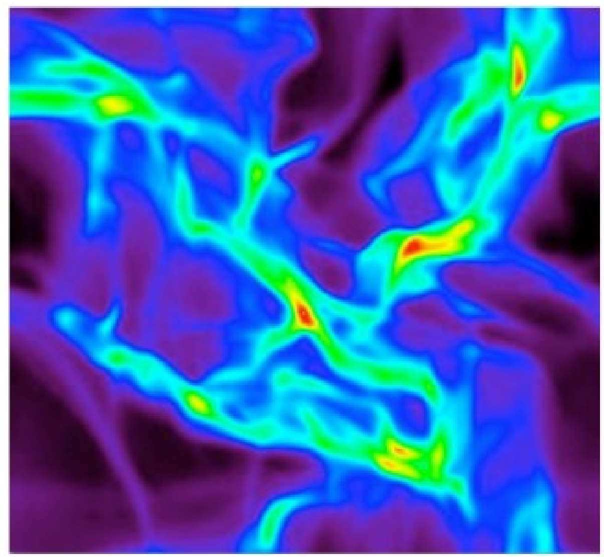

e.g. Padoan et al. (2001), Pudritz & Kevlahan (2013)

Magnetic-field guided sheet formation

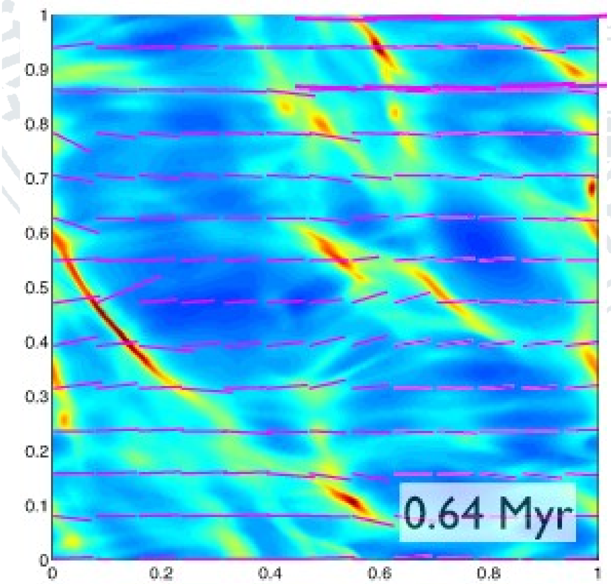

e.g. Chen & Ostriker (2014), Inutsuka et al. (2015)

- Filaments produced in many processes
- Distinguishable by ratio of sheets to filaments and velocity structure in filaments

Filaments

Observations

- Filaments everywhere

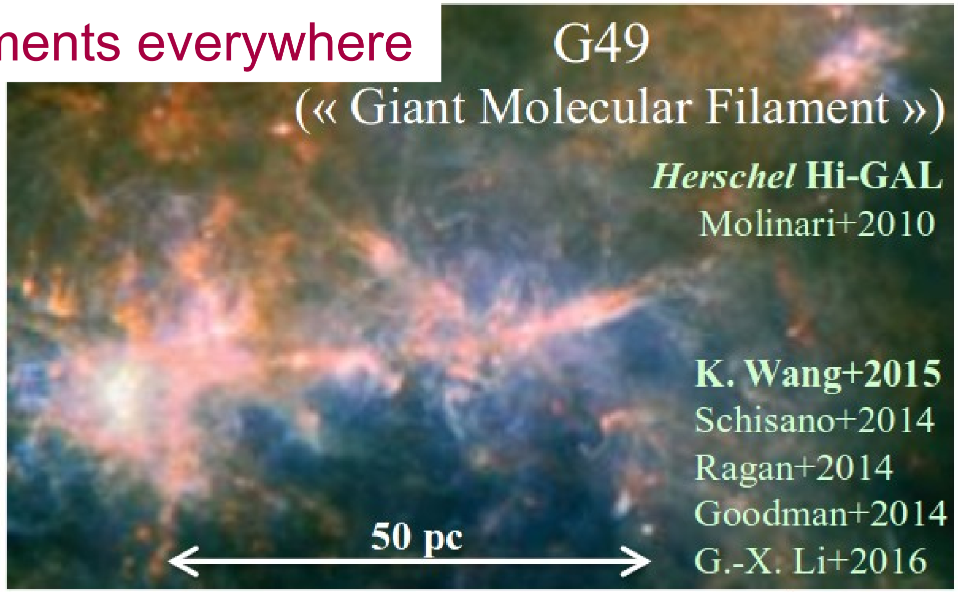

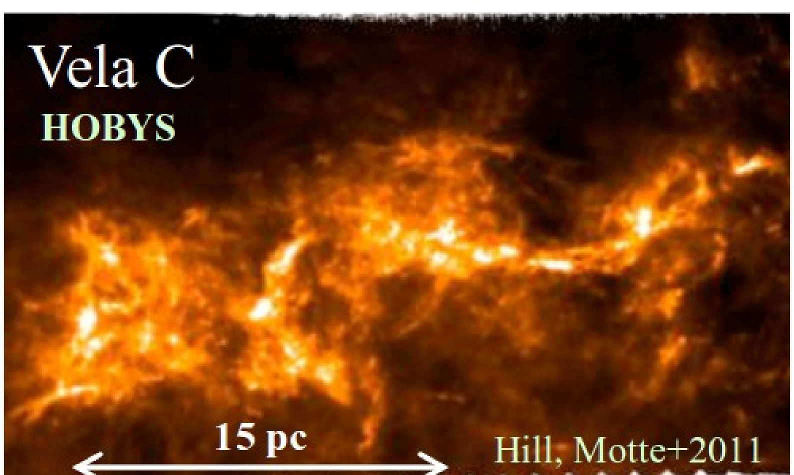

Ph. André - ISM2017 – Cologne– 13 Feb 2017

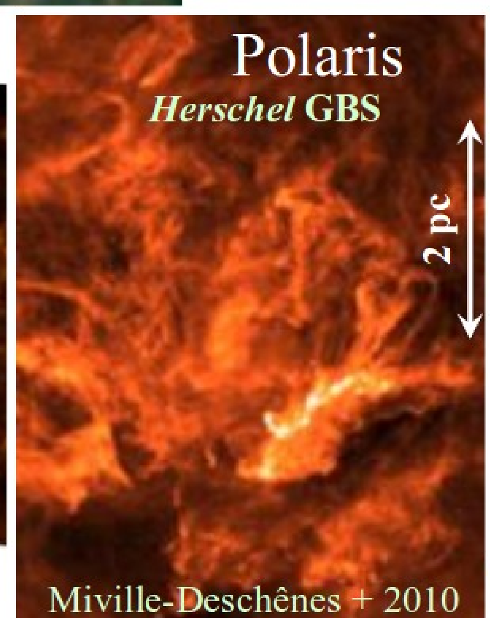

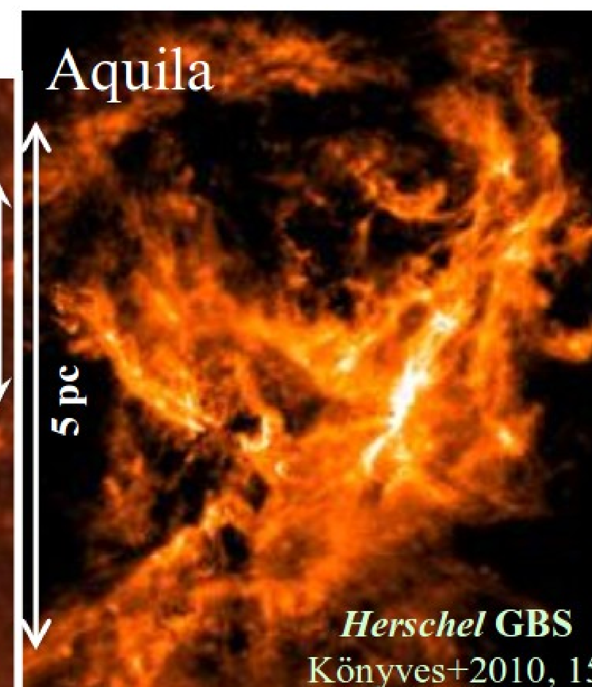

Filaments

Role

- Sites of star formation
  - Instable for $M/l > 16 M_\odot/\mathrm{pc}$

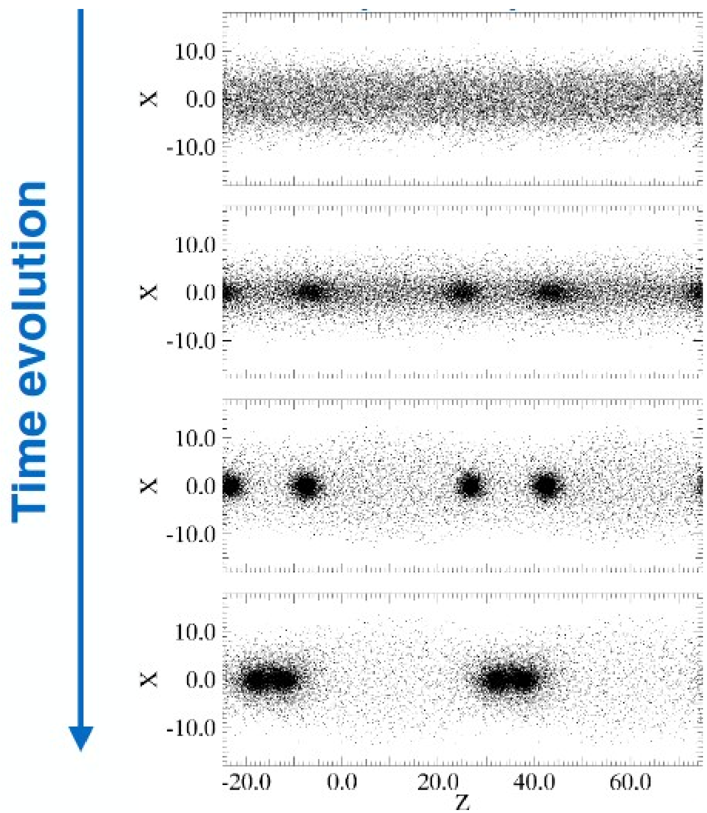

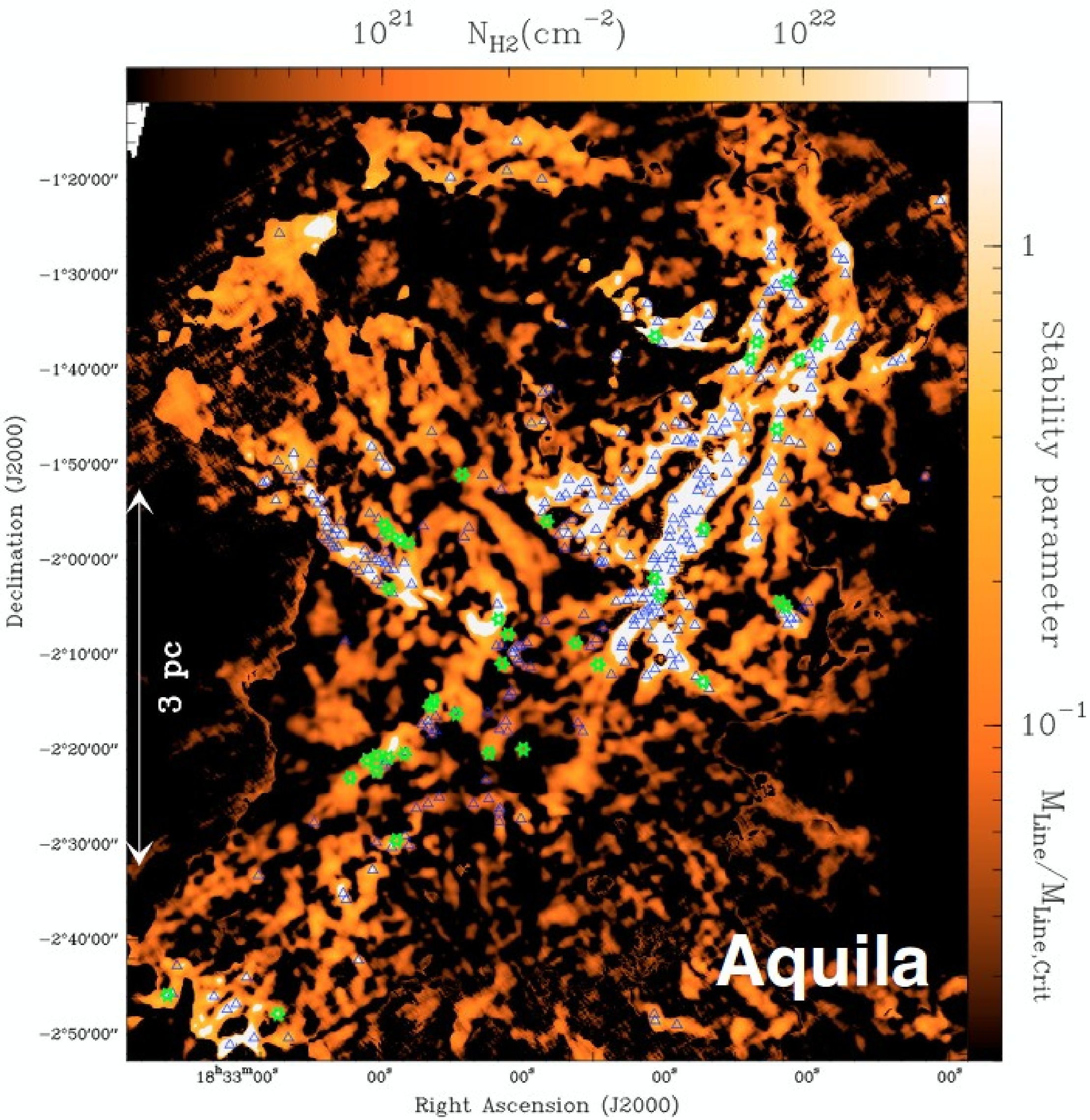

André et al (2010)

- Almost all prestellar and protostellar cores are found on filaments

Filaments

How to quantify filaments

- Traditional approach
  - Look for peaks in curvature space and connect them → DisPerSe, getFilaments

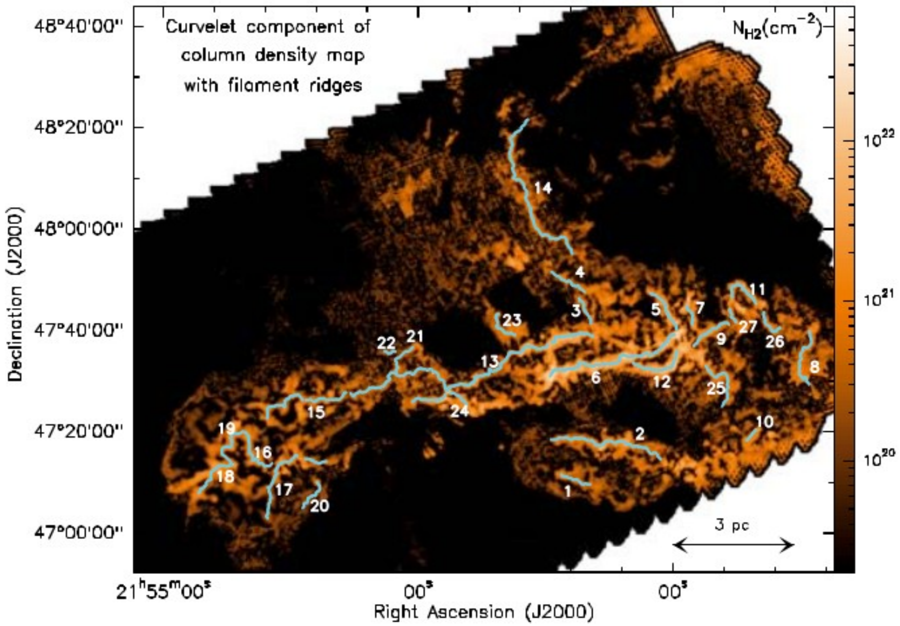

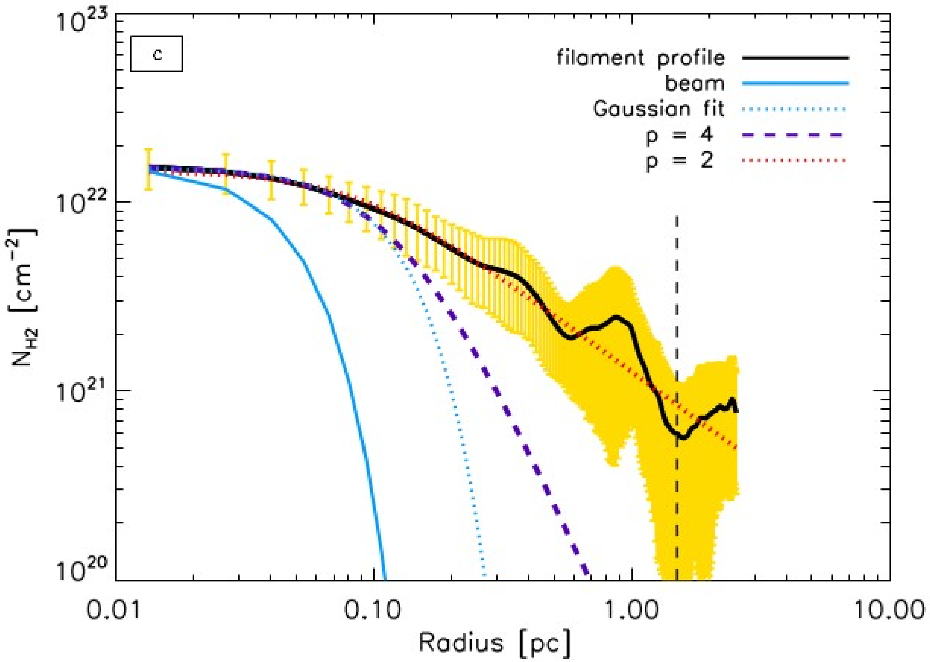

Arzoumanian et al. (2011)

  - Retrieves typical filament width (0.1pc) determined by scale/resolution used in the method (Panopoulou 2016), not by the underlying structure
  - Unbiased method required!

Wavelet based measure

- Convolution of the map $f(\mathbf{x})$: $W(s,\varphi,\mathbf{x}) = \frac{1}{s^{3/2}} \int_{-\infty}^{+\infty} \int_{-\infty}^{+\infty} f(\mathbf{x}) \psi_\varphi \left(\frac{\mathbf{x}' - \mathbf{x}}{s} \right) d\mathbf{x}'$

  with an anisotropic filter:

$$\psi(x,y) = \left[\exp(2\pi \imath x) - \exp(-\pi^2 b^2)\right] \exp\left(\frac{-x^2 - y^2}{b^2}\right)$$

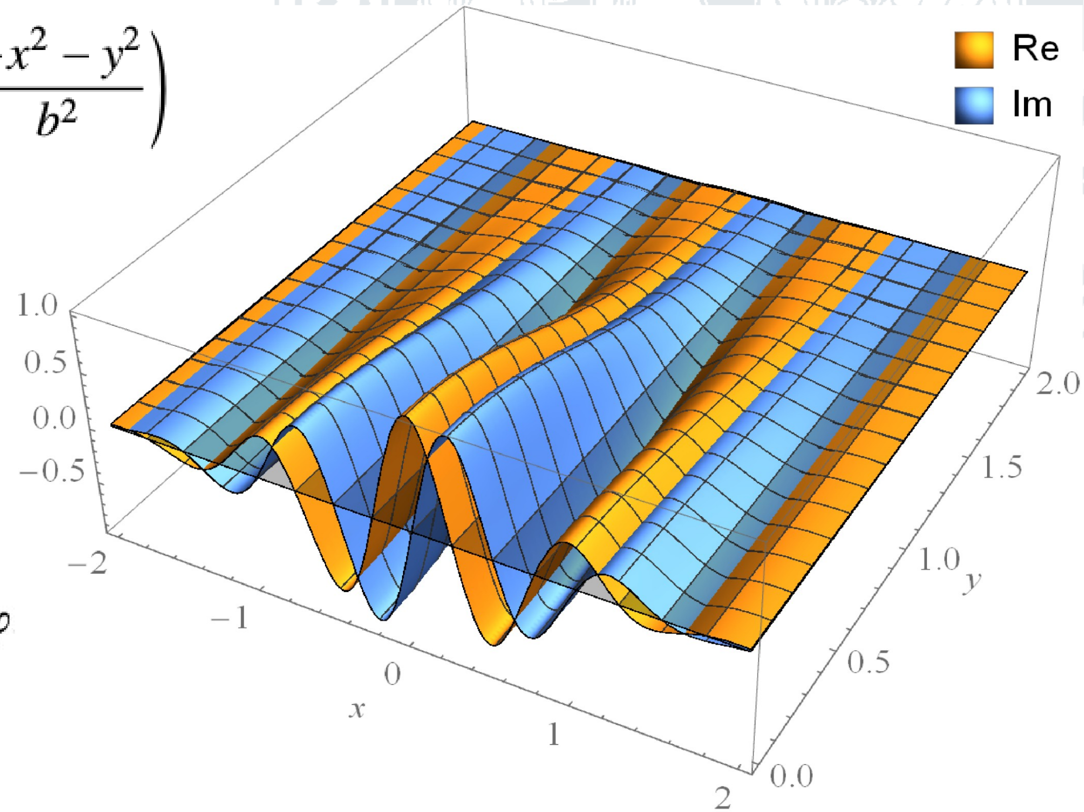

- Compute spectra of isotropic and anisotropic wavelet coefficients as a function of the filter size *s*:

$$m^i(s,\mathbf{x}) = (2\pi)^{-1} \int_{-\pi}^{+\pi} |W(s,\varphi,\mathbf{x})|^2 d\varphi,$$

$$m^a(s,\mathbf{x}) = (2\pi)^{-1} \int_{-\pi}^{+\pi} |W(s,\varphi,\mathbf{x})|^2 e^{2\imath\varphi} d\varphi$$

- Provides
  - spatial and angular distribution of the wavelet coefficients
  - local and global degree of anisotropy as a function of the size scale

Magnetohydrodynamic models

- Gas motion couples to magnetic field
- Different modes of wave propagations
- Large-scale asymmetries
- Filaments everywhere

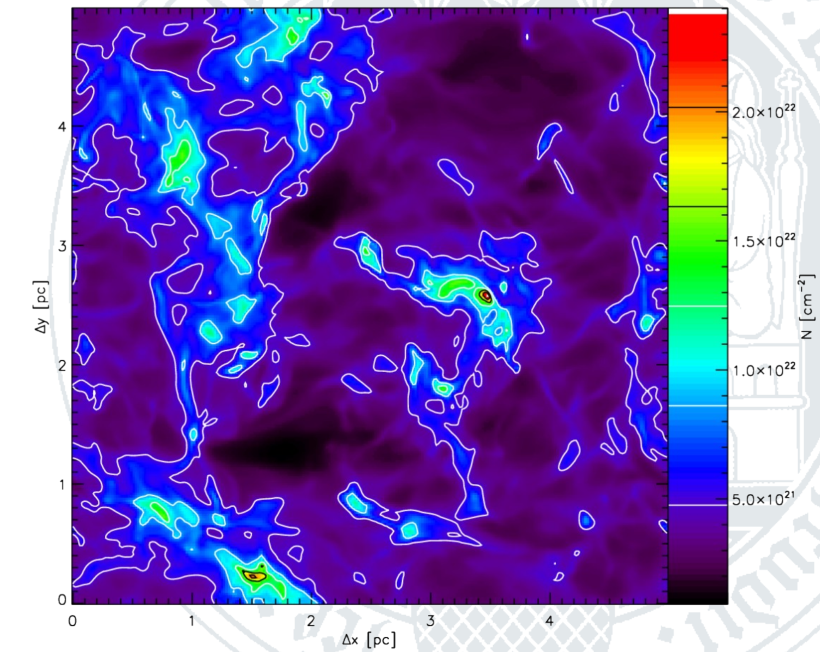

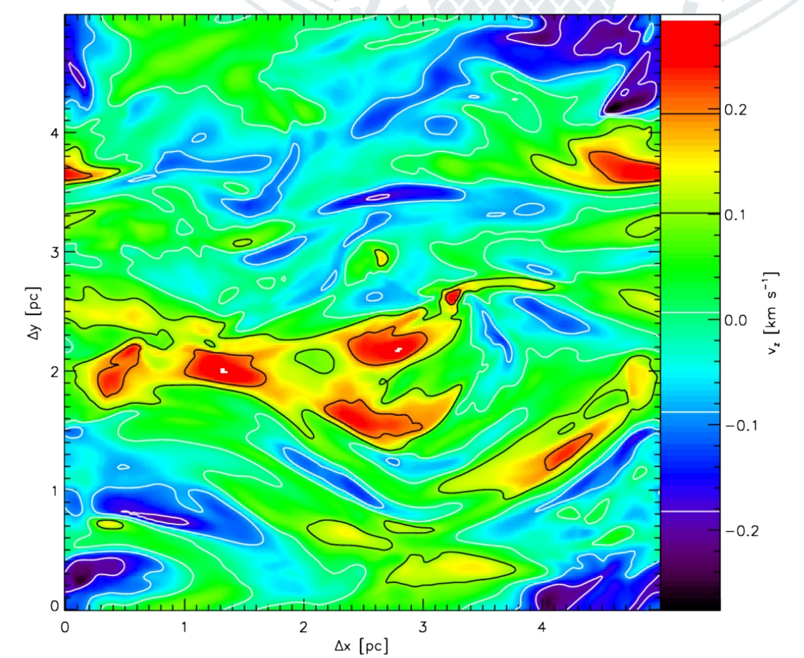

Column density structure and velocity slice in a supersonic, subalfvenic turbulence simulation (Burkhart et al. 2013)

Analysis of observable maps

Simulated CO 2-1 intensity maps from the MHD simulation using different optical depths:

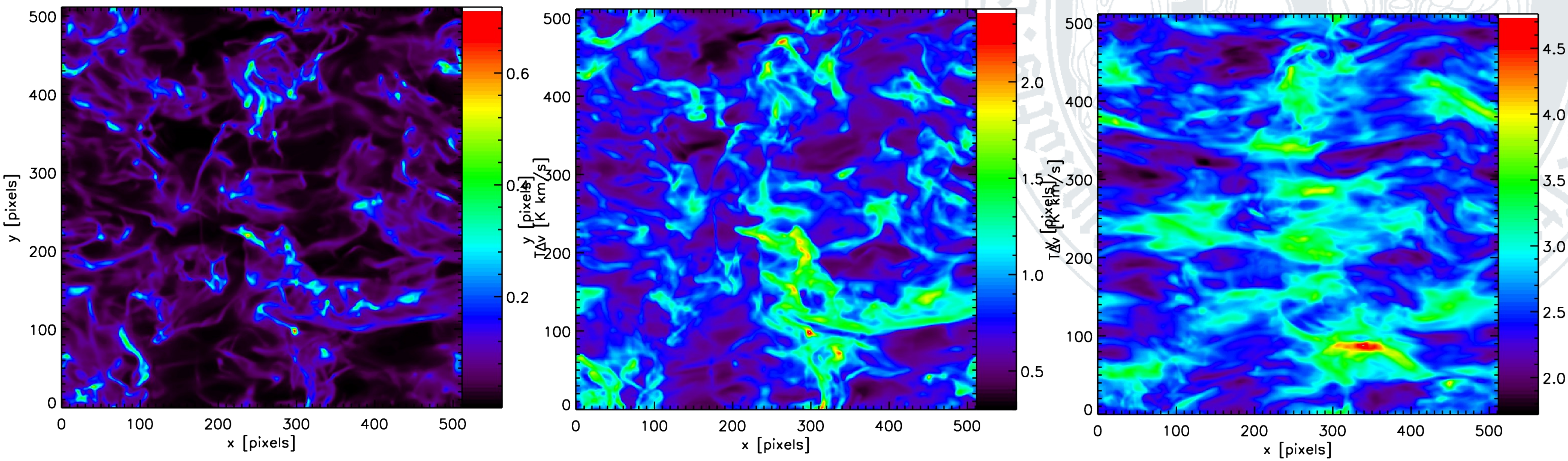

Different optical depth resulting from different molecular abundances:
$C^{18}O$: X=5 10^{-8}, ^{13}CO: X=1.5 10^{-6}, ^{12}CO: X=4.5 10^{-5}.

- All maps filamentary
- High optical depths emphasize the global anisotropy created by the magnetic field and imprinted mainly on the velocity field

Application to MHD simulations

Degree of anisotropy as a function of size scale:

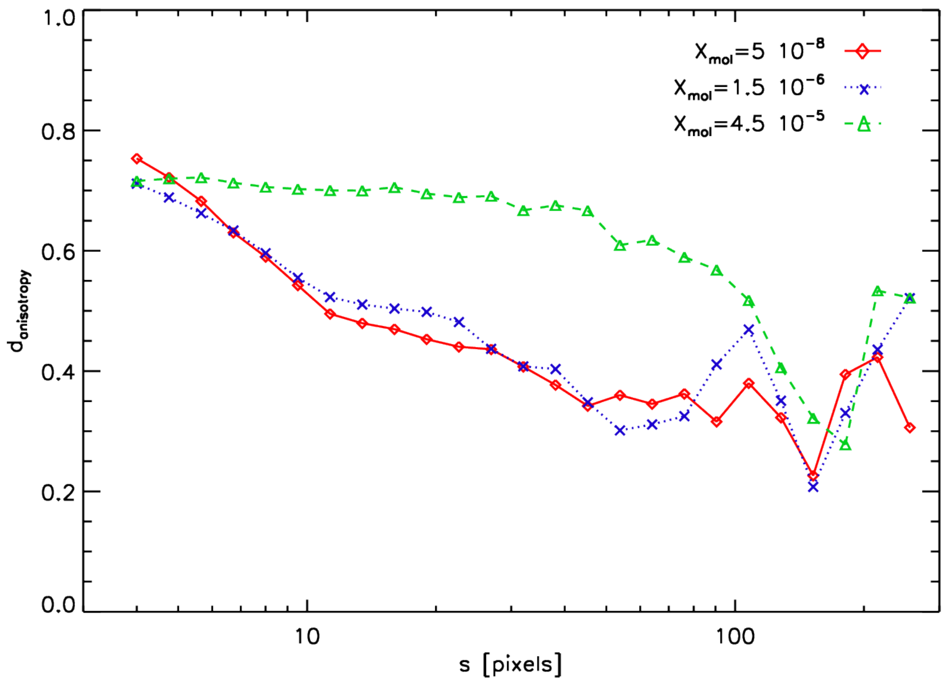

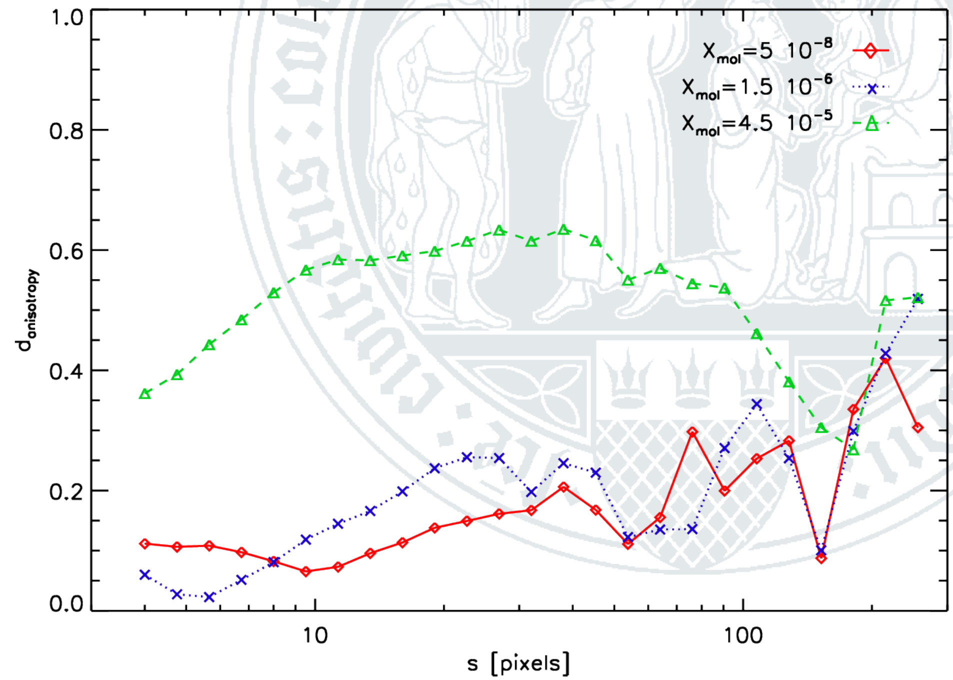

Spectra of the local (left) and global degree of anisotropy (right) for the three maps.

- The small filaments give a high degree of local anisotropy at small scales.
- For large optical depths the global anisotropy becomes significant. We find wider filaments. Filaments at low optical depth are unaligned.
- We see the imprint of the magnetic field on the structure at all size scales. Small-scale filaments are entangled with the field lines.

Application to observations

Column density maps from Herschel dust observations:

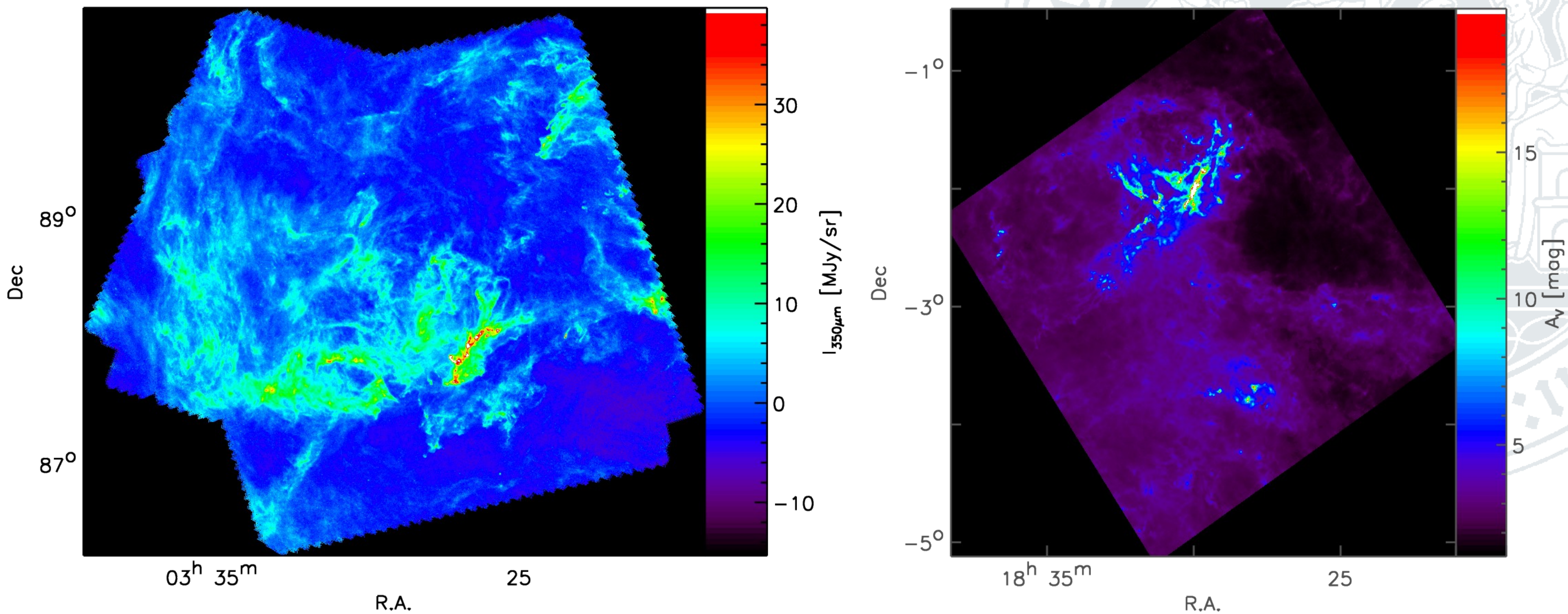

Filamentary dust maps of the Polaris (left) and Aquila (right) regions previously analysed by André et al. (2010). Pixel scale of 0.0075pc

- In spite of the different nature of the clouds André et al. (2010) find a common filament width of 0.1pc for both clouds.

Example: Polaris

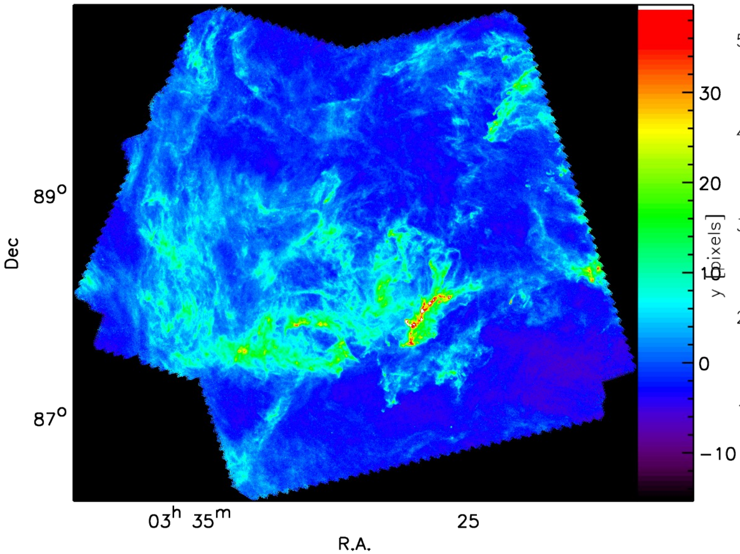

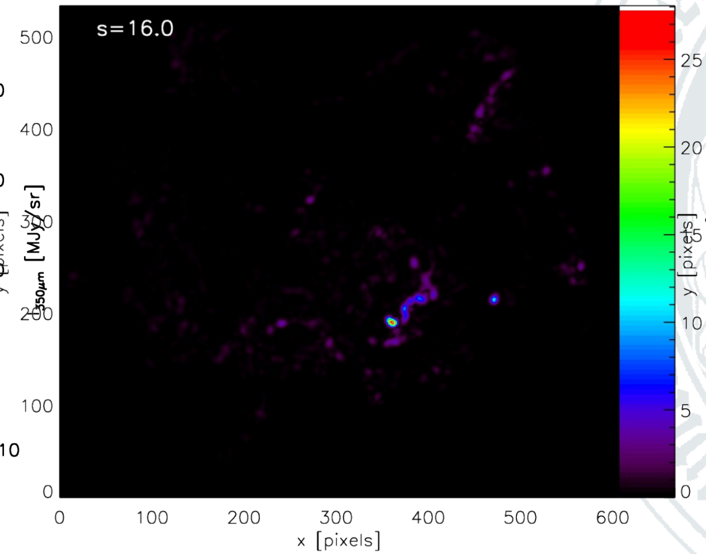

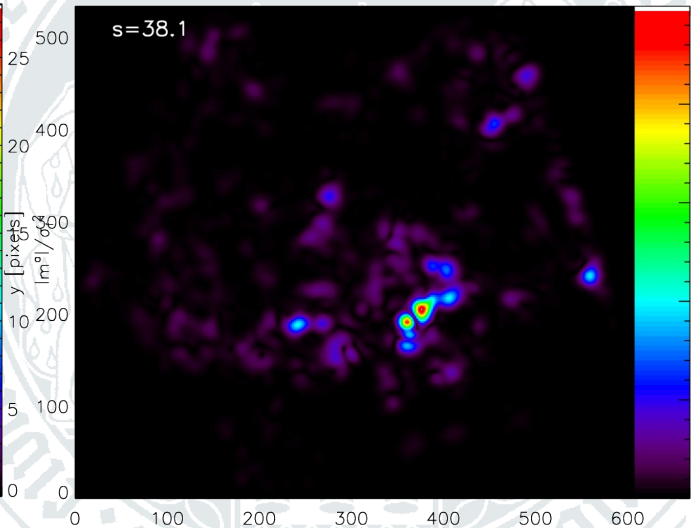

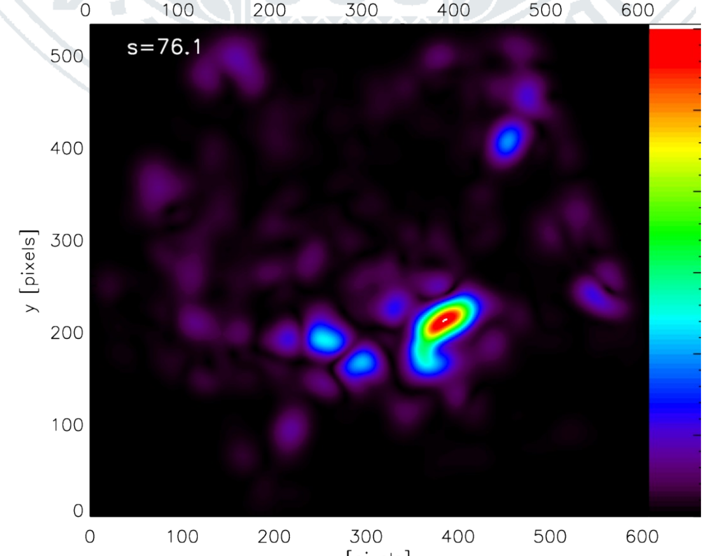

Maps of anisotropic wavelet coefficients for three different wavelet sizes:
16 pixels = 0.12pc,
38 pixels = 0.29pc,
76 pixels = 0.57pc

- The maps of wavelet coefficients follow the spines of the filaments identified by eye or one of the traditional filament finders

Anisotropic wavelet analysis

Application to observations

Wavelet spectra and degrees of anisotropy for both regions:

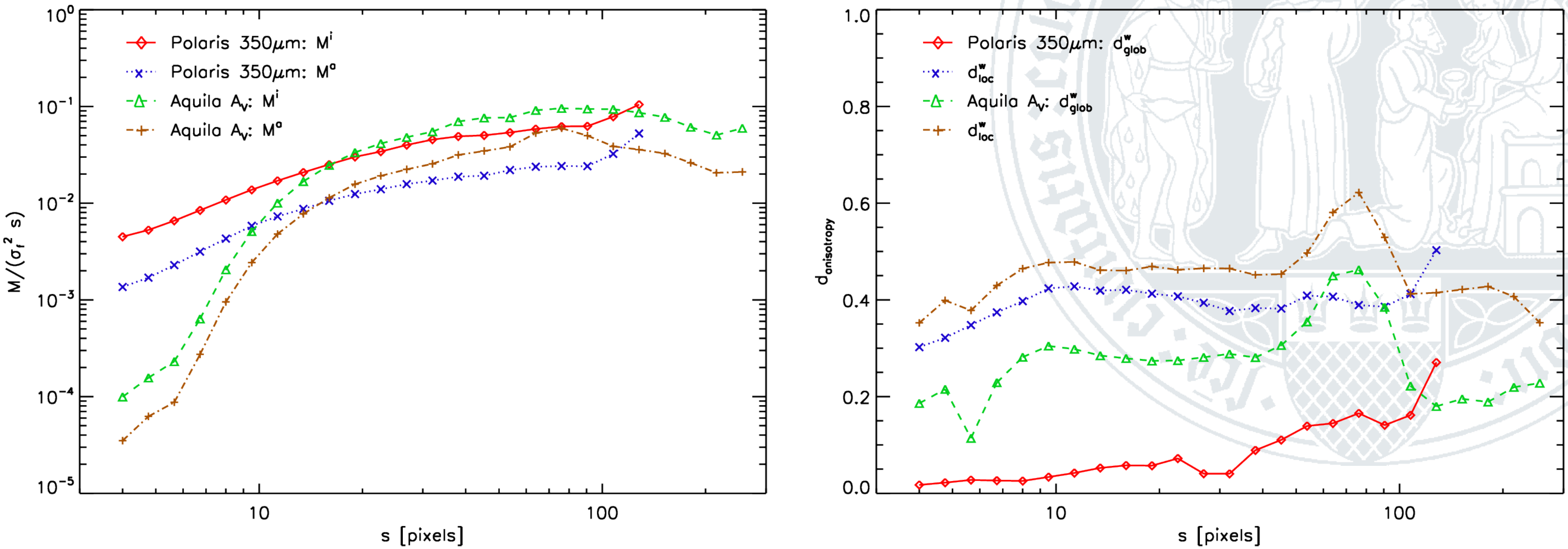

Isotropic and anisotropic wavelet coefficients (left) and local and global degrees of anisotropy (right) for the two maps.

- Polaris shows no characteristic size scale and no global anisotropy, but a high filamentariness measured by the local anisotropy at all scales.
- Aquila has two characteristic scales around 0.08 and 0.55pc and the filaments show global anisotropy.

Conclusion

We still do not understand interstellar turbulence!

We need a new cycle of:

- creating models
  - larger dynamic range of turbulence
  - physics of dissipation
  - self-consistent energy balance
  - chemical structure
- running radiative transfer computations
- measuring statistical properties and comparing them with observations.

Conclusions

Points we already learned:

- Turbulent structures are created in many ways, but
  - energy injection must occur on large (Galactic) scales, not outflows
  - simple gravity is in principle enough to explain all observed structures
  - magnetic fields are not dominant
  - clouds are neither stable nor stationary. Flow terms dominate.
- Many processes create filaments, but none produces fixed widths.
  - They occur for particular parameters and conditions only, e.g. magnetic field or radiative transfer effects.
  - By measuring the power in isotropic and anisotropic structures we get the relative importance of spherical and cylindrical collapse modes.
- Many clouds show two power law PDFs → some collapse threshold
  - Explanation ?????